Fundamentals of X-ray Absorption Fine Structure Spectroscopy

Sakura Pascarelli

European XFEL

sakura.pascarelli@xfel.eu

XVIII School on Synchrotron Radiation “Gilberto Vlaic”

Muggia, Italy , 21 September – 1 October 2026

Outline

10’ Break @ 17h10

- EXAFS: a probe of local structure
- EXAFS: simple theoretical description and derivation of EXAFS equation
- XANES: a probe of electronic structure and coordination chemistry
- Applications

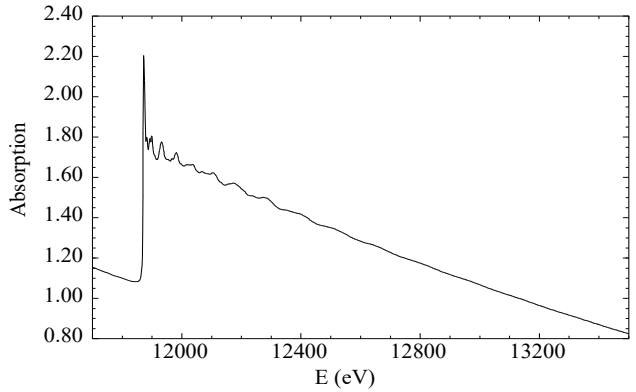

Outline

- EXAFS: a probe of local structure
- EXAFS: simple theoretical description and derivation of EXAFS equation
- XANES: a probe of electronic structure and coordination chemistry
- Applications

EXAFS qualitatively

Absorption coefficient = probability of photon absorption
~ probability of electron presence at origin = "amount of wave" at origin

isolated atom

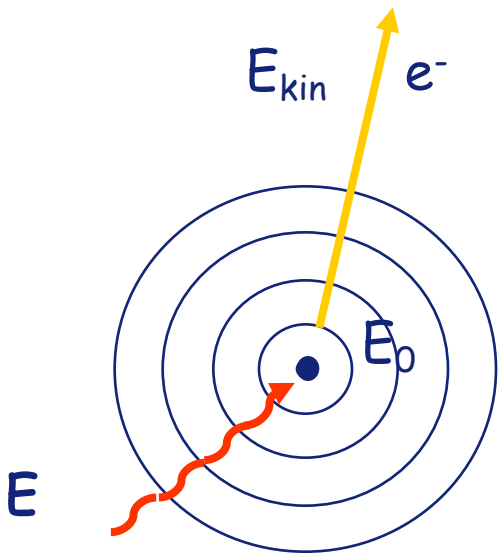

condensed matter

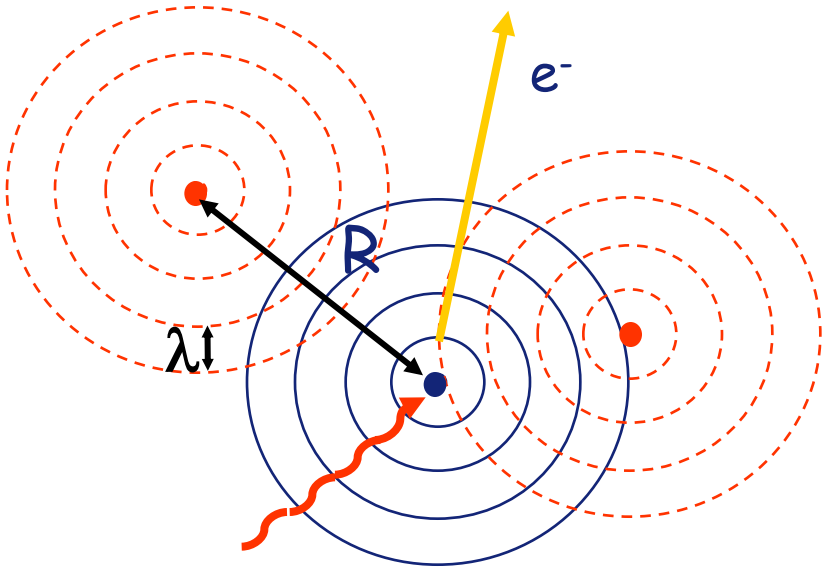

The kinetic energy of the ejected photoelectron E_{kin} is:

$$E_{kin} = E - E_0 = \frac{p^2}{2m} = \frac{\hbar^2 k^2}{2m}$$

$\lambda = 2\pi/k$

Where do the oscillations come from?

Due to a quantum effect, the autointerference of photoelectron wave modifies the absorption coefficient value:

$$E_{kin} = E - E_0 = \frac{p^2}{2m} = \frac{\hbar^2 k^2}{2m}$$

1. As E is scanned above E_0, E_{kin} is varied, and consequently k and λ.

2. The outgoing and backscattered parts of the wave interfere either constructively or destructively, depending on the ratio between λ and R.

3. It is the interference between outgoing and incoming waves that gives rise to the sinusoidal variation of μ(E)

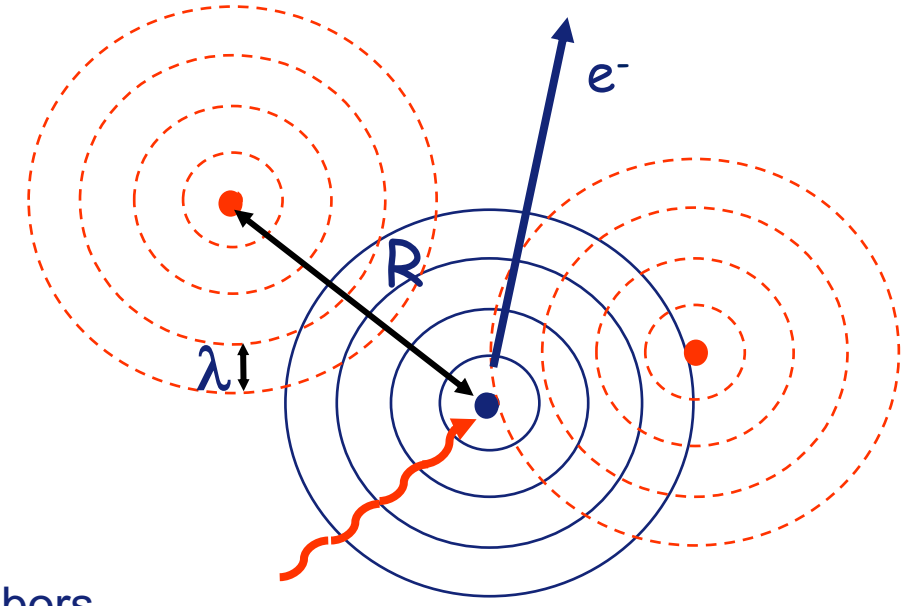

- frequency ~ distance from neighbors
- amplitude ~ number and type of neighbors

X-RAY ABSORPTION FINE STRUCTURE: EXAFS

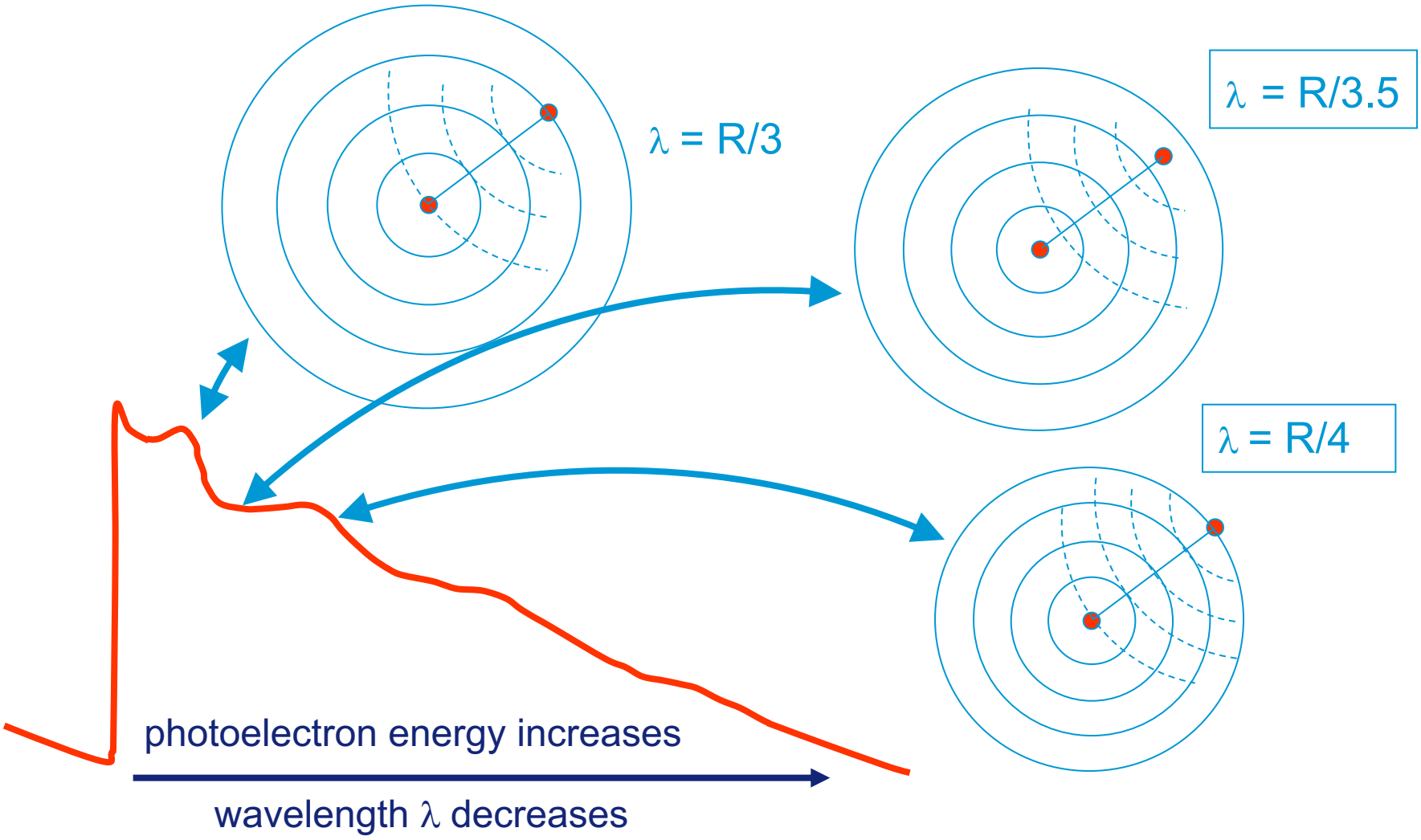

The probability of absorption oscillates due to constructive and destructive interference

The EXAFS signal χ

We're interested in the energy dependent oscillations in μ(E), as these will tell us something about the neighboring atoms, so we define the EXAFS as:

$$\chi(E) = \frac{\mu(E) - \mu_0(E)}{\Delta\mu_0(E_0)}$$

We subtract off the smooth "bare atom" background $\mu_0(E)$, and divide by the edge step $\Delta\mu_0(E_0)$, to give the oscillations normalized to 1 absorption event.

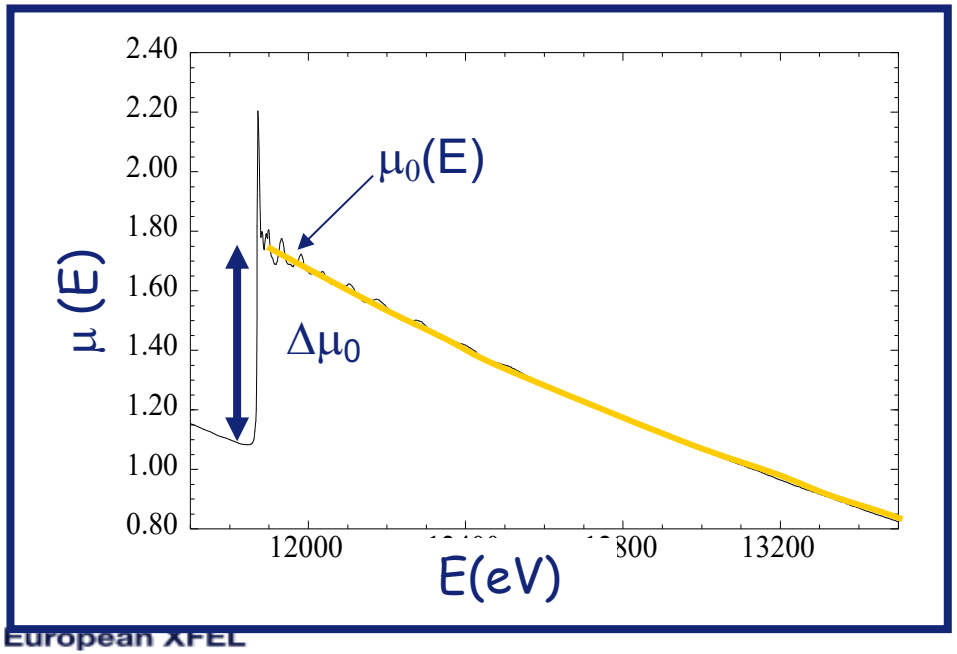

EXAFS: χ (k)

XAFS is an interference effect, and depends on the wave-nature of the photoelectron.

It's convenient to think of XAFS in terms of photoelectron wavenumber, k, rather than X-ray energy

$$k = \sqrt{\frac{2\,m\,(E - E_0)}{\hbar^2}}$$

χ (k) is often shown weighted by k^2 or k^3 to amplify the oscillations at high-k:

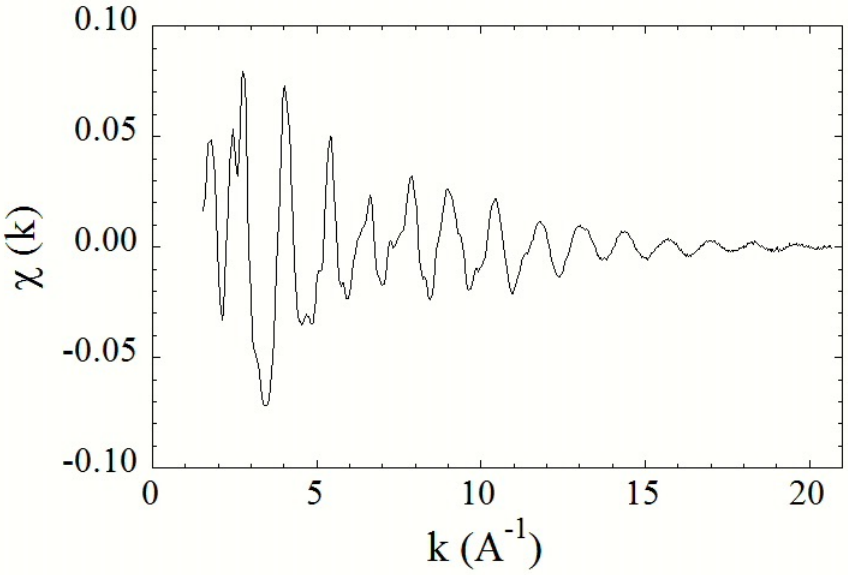

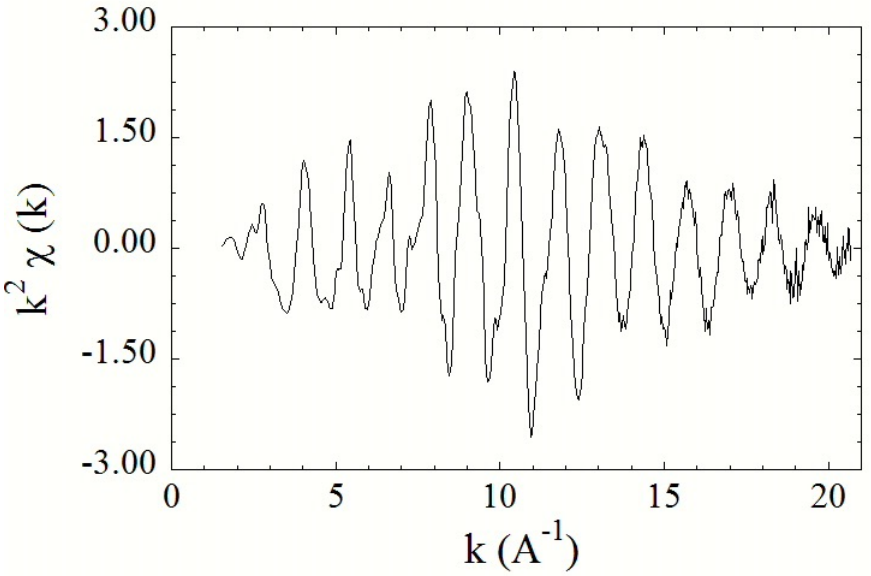

Qualitative picture of local coordination in R space

The frequencies contained in the EXAFS signal depend on the distance between the absorbing atom and the neighboring atoms (i.e. the length of the scattering path).

A Fourier Transform of the EXAFS signal provides a photoelectron scattering profile as a function of the radial distance from the absorber.

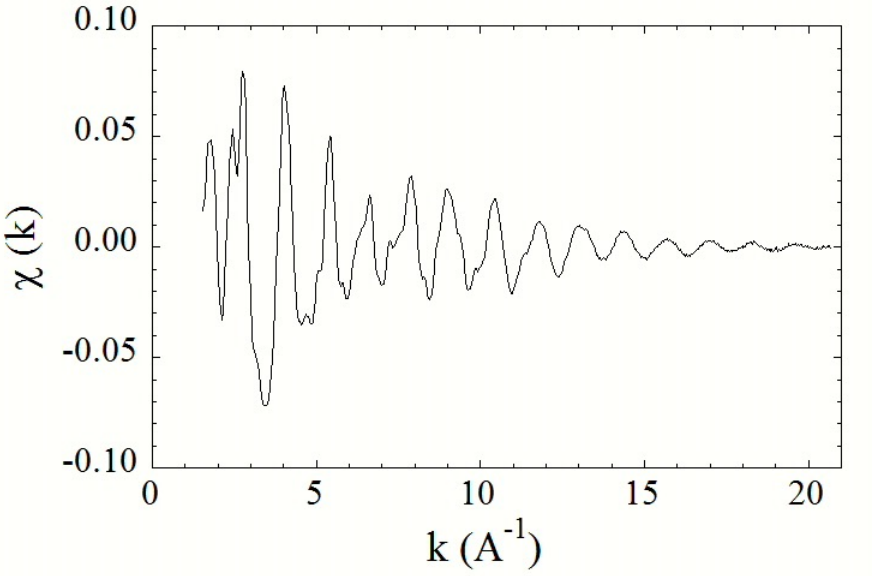

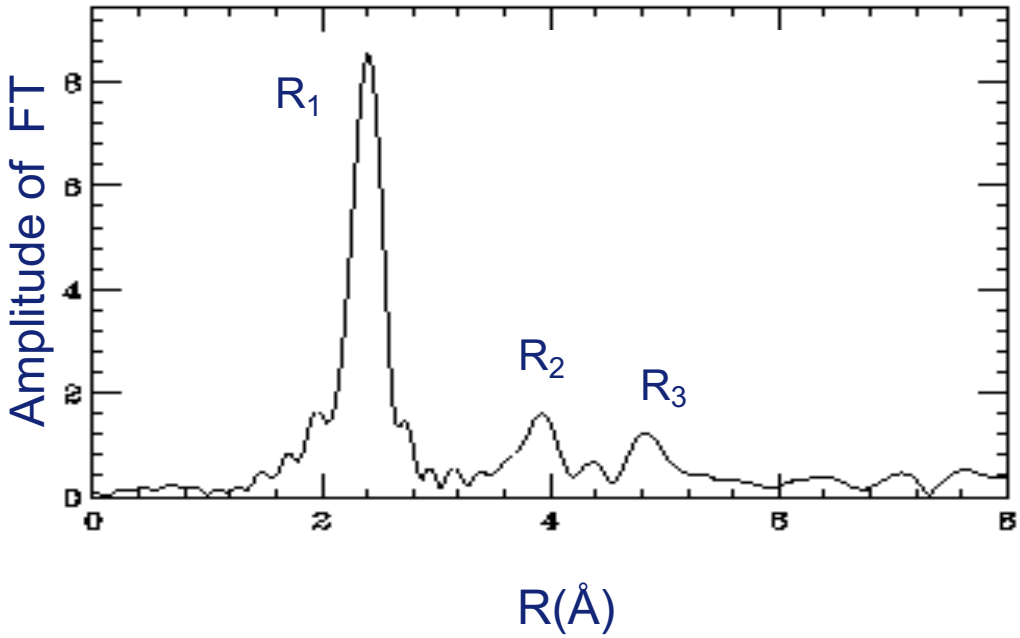

Quantitative structural determination

Structural determinations depend on the feasibility of resolving the data into individual waves corresponding to the different types of neighbors (SS) and bonding configurations (MS) around the absorbing atom.

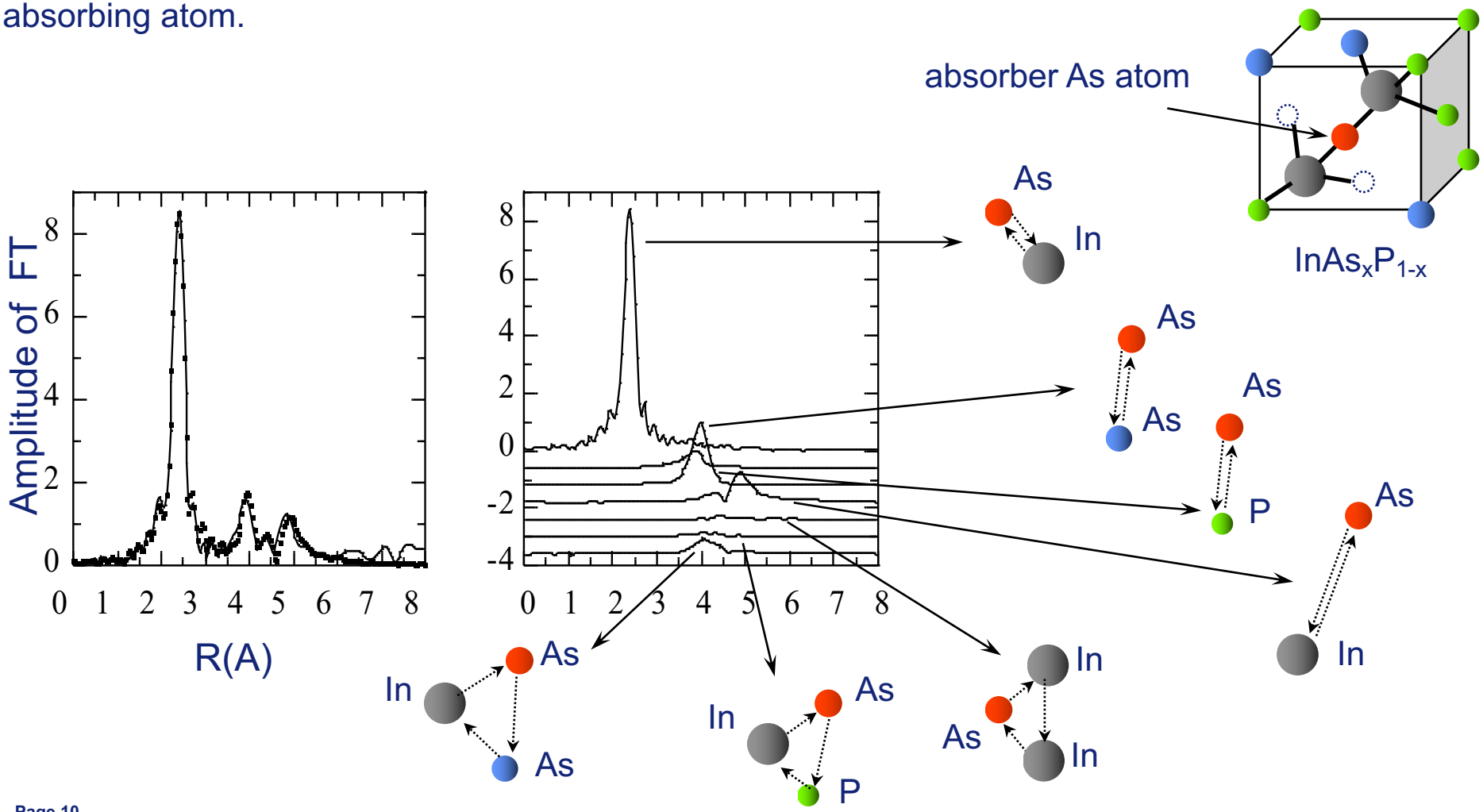

χ: sum of damped waves

χ (k) is the sum of contributions χ_j (k) from backscattered wavelets:

$$\chi(k) = \sum_j \chi_j(k)$$

Path expansion
- implies photoel w/short mean free path
- true only for EXAFS

Each χ_j (k) can be approximated by a damped sine wave of the type:

$$\chi_j(k) = A_j(k)\sin[\varphi_j(k)]$$

$$N_j f_j(k) e^{-2k^2\sigma^2}$$

The larger the number of neighbors, the larger the signal

The stronger the scattering amplitude, the larger the signal

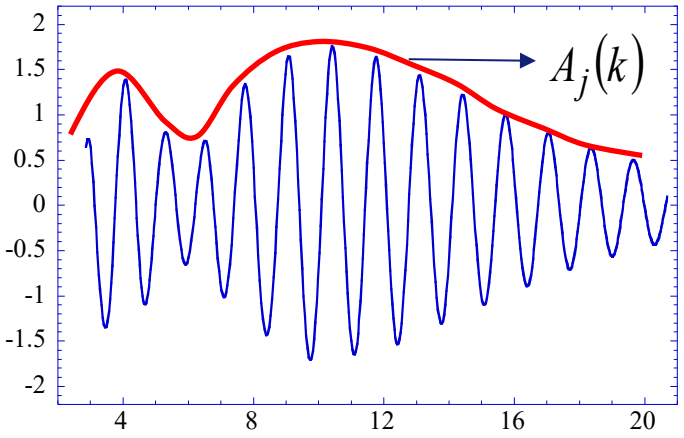

Damping of the amplitude at large k, due to static and thermal disorder

$$2kR_j + \delta_j(k)$$

Each shell contributes a sinusoidal signal which oscillates more rapidly the larger the distance

Frequencies: Single and Multiple Scattering paths

The sum over paths in the EXAFS equation includes many shells of atoms (1st neighbor, 2nd neighbor, 3rd neighbor, . . .), but can also include multiple scattering paths, in which the photoelectron scatters from more than one atom before returning to the central atom.

SS ⇨ $g_2(r)$ $f = 2\,R_1$

MS ⇨ $g_2(r)$ $f = 4\,R_1$

MS ⇨ $g_3(r)$ $f = R_1 + R_2 + R_3$

MS ⇨ $g_3(r)$ $f = 2R_1 + 2R_3$

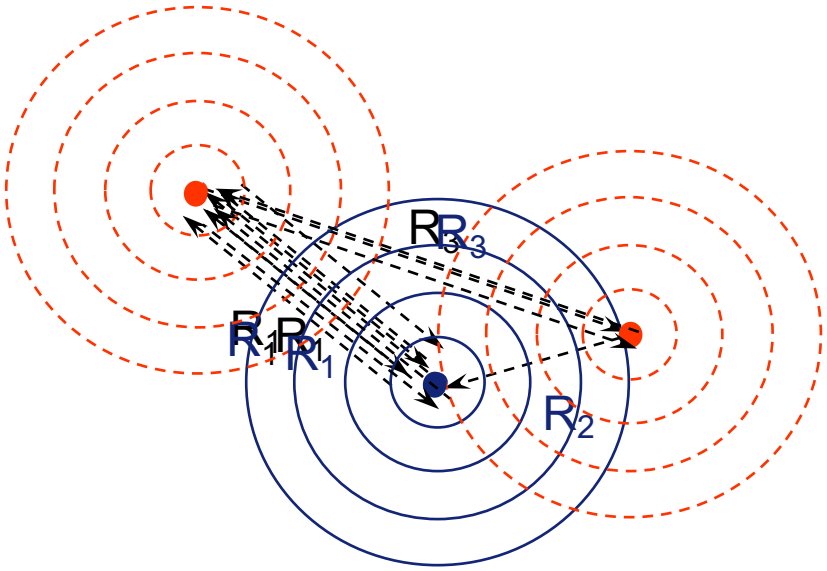

EXAFS can give information on the n-body distribution functions $g_n(r)$.

Amplitudes

$$A_j(k) \sim N_j f_j(k) e^{-2k^2\sigma^2}$$

absorber As atom

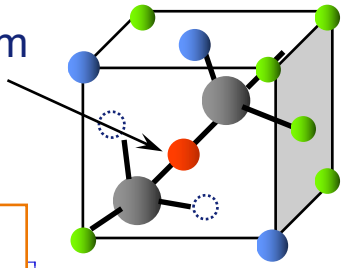

$InAs_xP_{1-x}$

shape of the envelope of each wave indicative of nature of backscatterer atom:

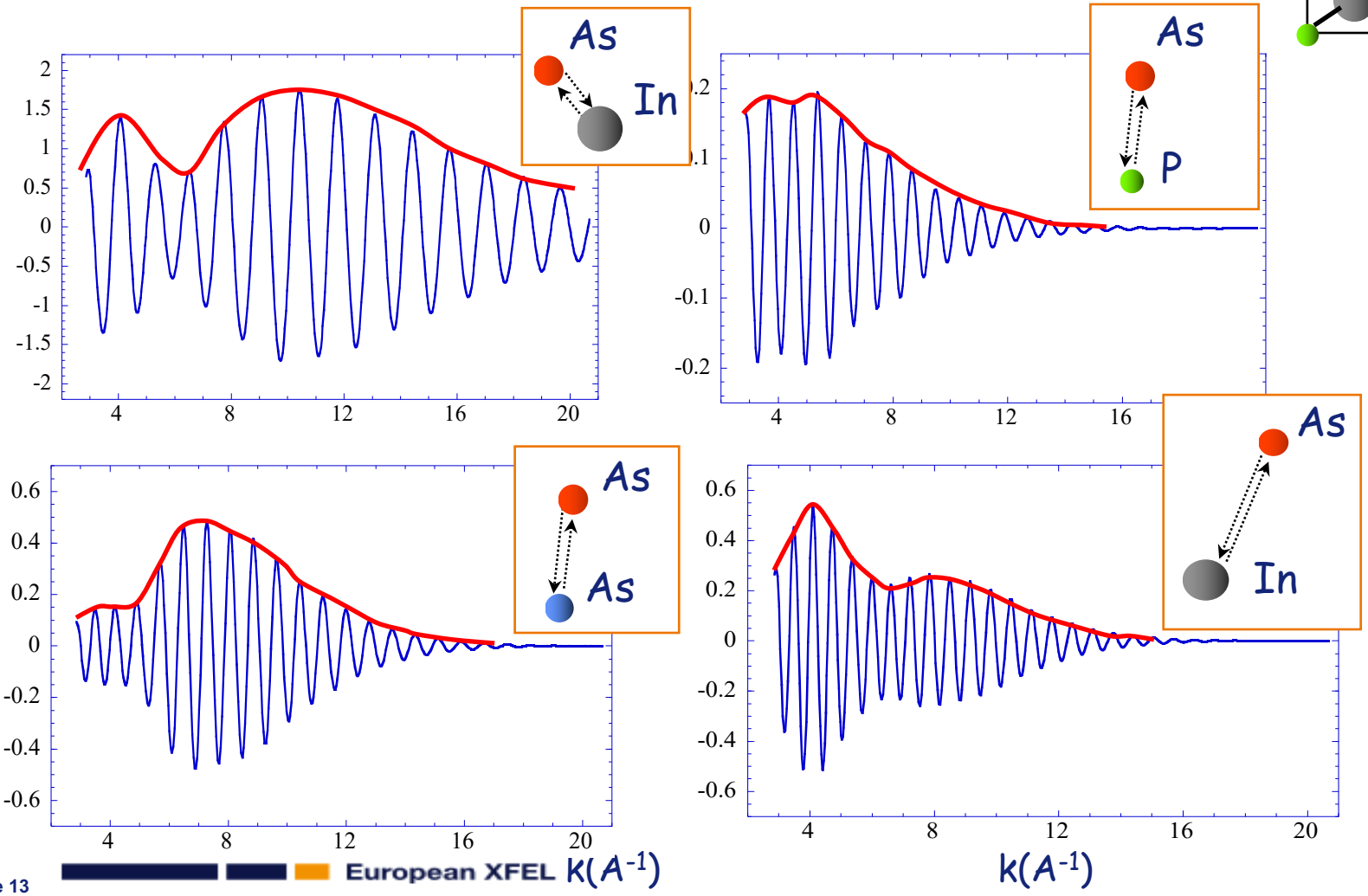

Scattering Amplitude and Phase-Shift: f (k) and δ (k)

The scattering amplitude f (k) and phase-shift δ (k) depend on atomic number.

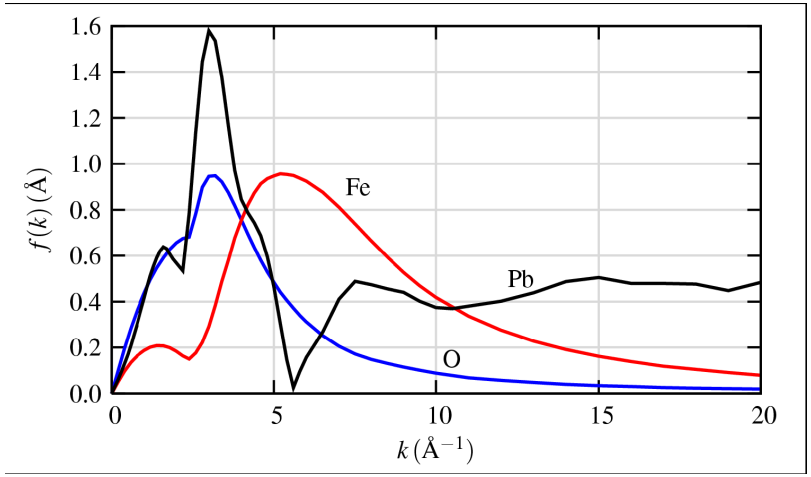

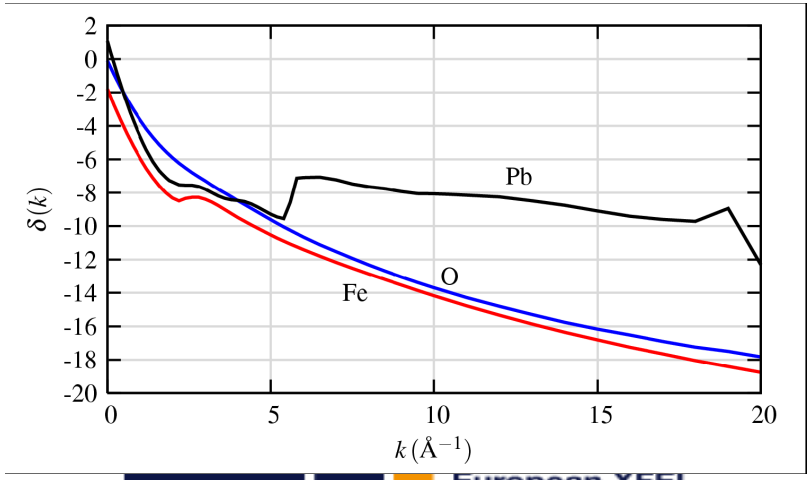

The scattering amplitude f (k) peaks at different k values and extends to higher-k for heavier elements. For very heavy elements, there is structure in f (k).

The phase shift δ(k) shows sharp changes for very heavy elements.

These scattering functions can be accurately calculated (i.e. with the programs FEFF, GNXAS, etc.), and used in the EXAFS modeling.

Z can usually be determined to within 5 or so. Fe and O can be distinguished, but Fe and Mn cannot be.

Calculating f (k) and δ (k)

These days, we can calculate f (k) and δ (k) easily using different software codes.

These programs take as input:

1. a list of atomic x,y,z coordinates for a physical structure
2. a selected central atom

The result is a set of files containing the f (k), and δ (k) for a particular scattering "shell" or "scattering path" for that cluster of atoms.

Many analysis programs use these files directly to model EXAFS data.

A structure that is close to the expected structure can be used to generate a model, and used in the analysis programs to refine distances and coordination numbers.

Outline

- EXAFS: a probe of local structure
- EXAFS: simple theoretical description and derivation of EXAFS equation
- XANES: a probe of electronic structure and coordination chemistr
- Applications

SIMPLE THEORETICAL DESCRIPTION

Kr gas

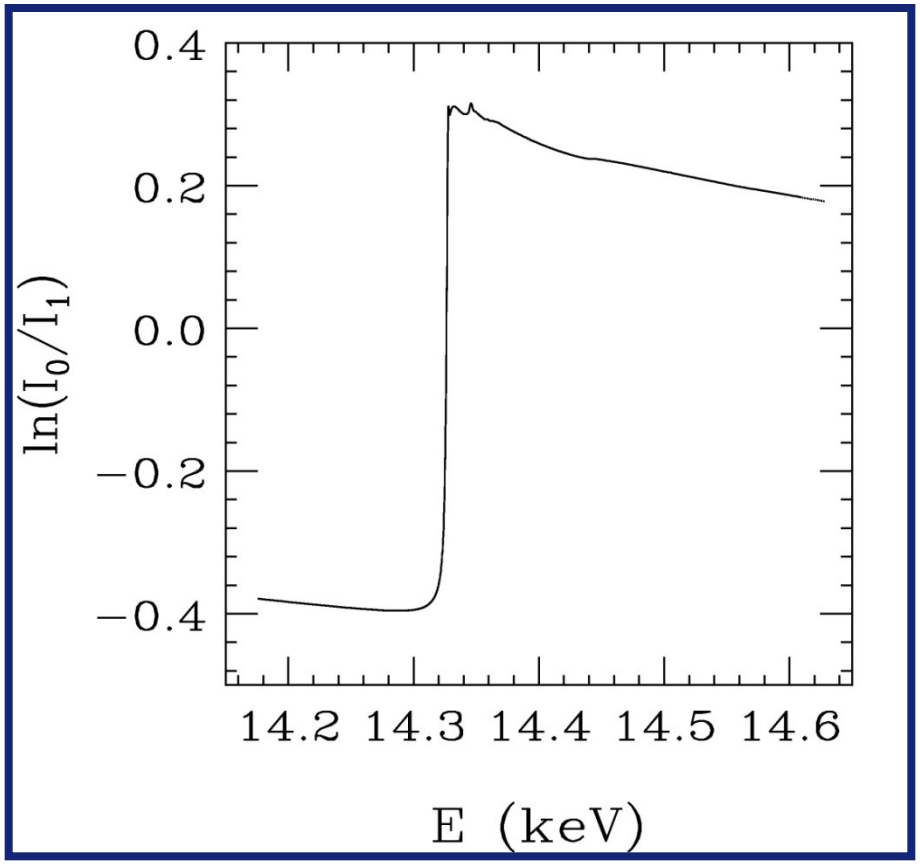

Rh metal

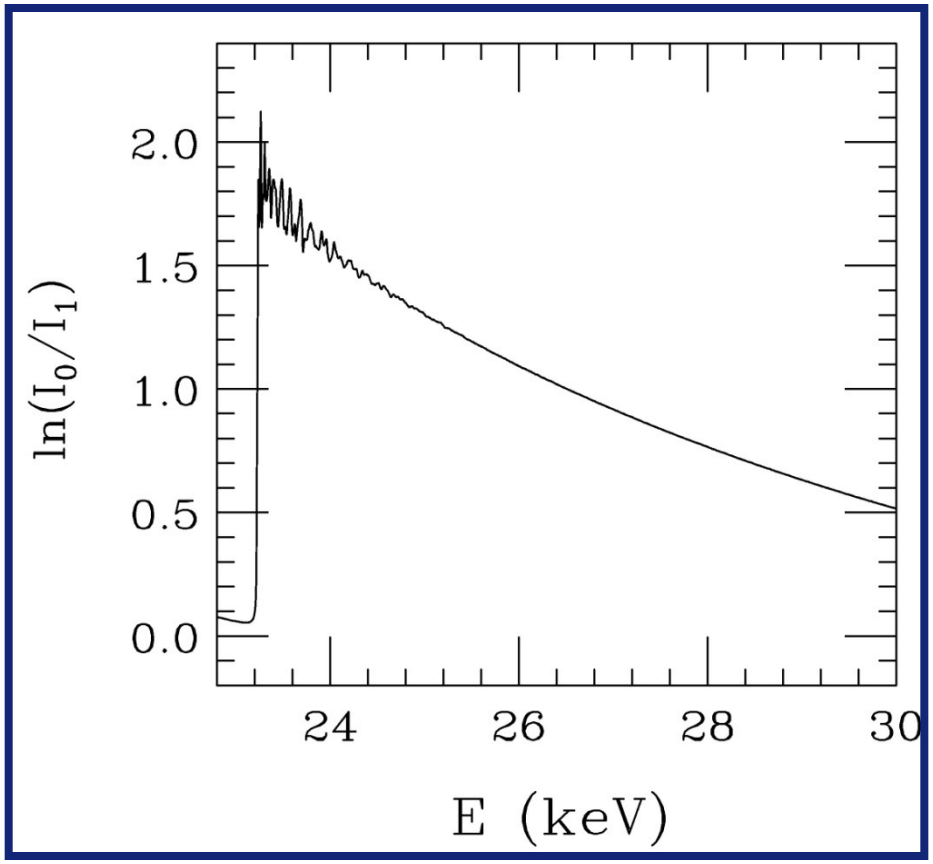

WAVEFUNCTIONS AND PROBABILITY DENSITY

In quantum mechanics, we use the concept of wavefunction to describe the probability of finding a particle at position $\vec{r}$ and time t :

$$\psi(\vec{r},t)$$

This function represents a “probability amplitude” and is a complex number:

$|i\rangle \quad \psi_i(\vec{r})$ $\qquad$ $|f\rangle \quad \psi_f(\vec{r})$

$\langle i| \quad \psi_i^*(\vec{r})$ $\qquad$ $\langle f| \quad \psi_f^*(\vec{r})$

The modulus squared of this quantity represents a probability or probability density:

$$\left|\psi_i(\vec{r})\psi_i^*(\vec{r})\right| = \left|\psi_i(\vec{r})\right|^2 \qquad \text{where :} \qquad \left|\int d\vec{r}\ \psi_i(\vec{r})\psi_i^*(\vec{r})\right|^2 = 1$$

The notation: $\left|\langle f|\hat{H}_I|i\rangle\right|^2$ stands for : $\left|\int d\vec{r}\ \psi_f^*(\vec{r})\,\hat{H}_I\,\psi_i(\vec{r})\right|^2$

So, if $\hat{H}_I|i\rangle = |f\rangle$ then the transition probability from $|i\rangle$ to $|f\rangle$ is equal to 1.

Absorption coefficient

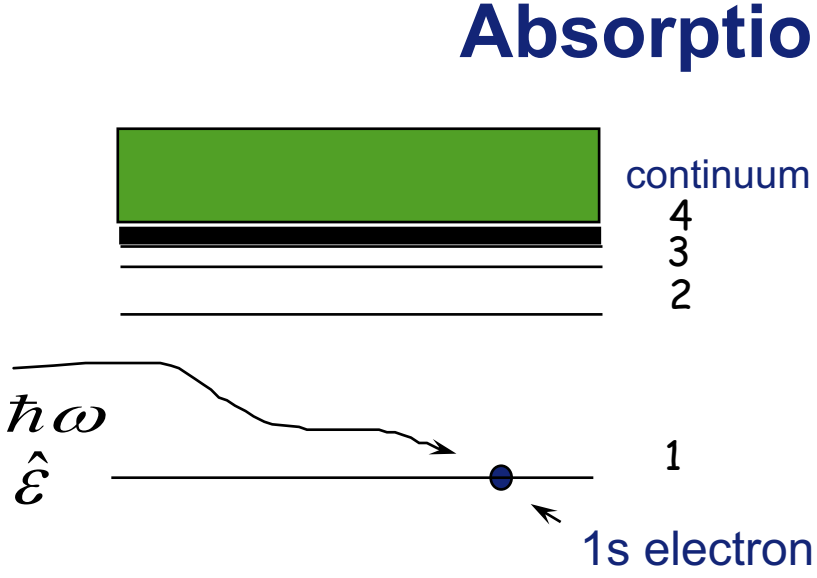

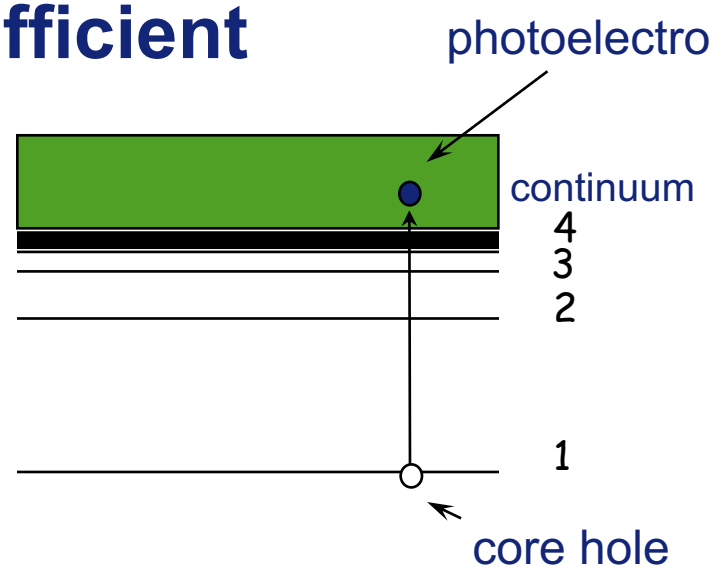

$$\mu(\omega) \approx \sum_f \left|\left\langle \Psi_f \left| \hat{H}_I \right| \Psi_i \right\rangle\right|^2 \approx \sum_f \left|\left\langle \Psi_f \left| \hat{\varepsilon}\cdot\hat{r} \right| \Psi_i \right\rangle\right|^2$$

dipole

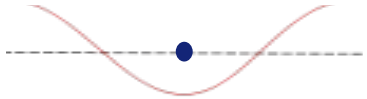

$$\hat{H}_I \approx \sum_j \vec{A}(\vec{r}_j)\cdot\vec{\nabla}_j$$

$$\approx A_0 \sum_j \hat{\varepsilon}\cdot\vec{\nabla}_j \approx A_0 \sum_j \hat{\varepsilon}\cdot\vec{r}_j$$

in principle, all electrons are involved → multi body process

$$\approx \sum_f \left|\left\langle \Psi_f^{N-1}\psi_f \left| \hat{\varepsilon}\cdot\vec{r} \right| \Psi_i^{N-1}\psi_i \right\rangle\right|^2 \approx S_0^2 \sum_f \left|\left\langle \psi_f \left| \hat{\varepsilon}\cdot\vec{r} \right| \psi_i \right\rangle\right|^2$$

single electron

sudden

$$S_0^2 \approx \sum_f \left|\left\langle \Psi_f^{N-1} \middle| \middle| \Psi_i^{N-1} \right\rangle\right|^2$$

[Appendix 1 & 2 for more info]

SIMPLE THEORETICAL DESCRIPTION

$$\mu(\omega) \approx \sum_f \left| \langle \psi_f | \hat{\varepsilon} \cdot \vec{r} | \psi_i \rangle \right|^2$$

$$\underbrace{\delta(m_s', m_s)}_{\text{spin}} \underbrace{\langle R_{n',l}(r)|r|R_{n,c}(r)\rangle}_{\text{radial}} \underbrace{\sum_{m_c,m_l,p} e^q_{\alpha,p} \langle l, m_l | C^{(1)}_p | c, m_c \rangle,}_{\text{angular}}$$

matrix elements factor into spin, radial and angular parts

By looking at the non-zero matrix elements we get the dipole selection rules

$$\begin{aligned}
&\Delta l = l' - l = \pm 1, \\
&\Delta m_l = m_l' - m_l = q = 0, \pm 1, \\
&\Delta s = s' - s = 0, \\
&\Delta m_s = m_s' - m_s = 0.
\end{aligned}$$

where $q\hbar$ is the X-ray angular momentum

For 1-electron transitions:

edge	initial state ψ_i	final state ψ_f
K, L_1	s (l=0)	p (l=1)
L_2, L_3	p (l=1)	s (l=0), d (l=2)

Absorption coefficient

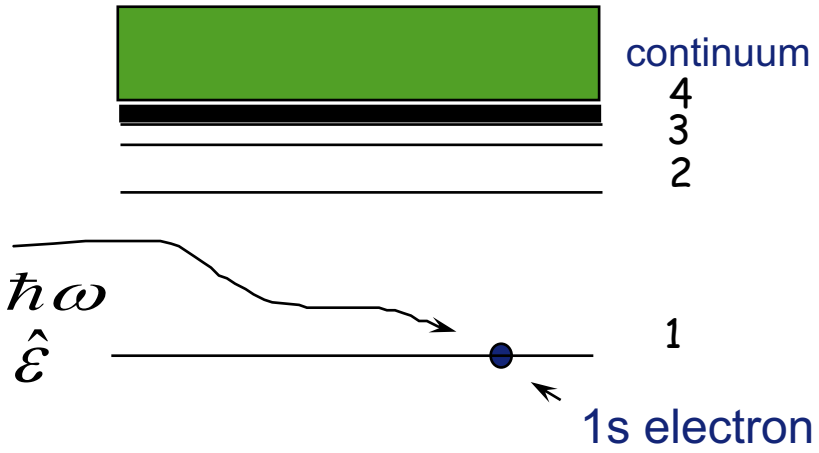

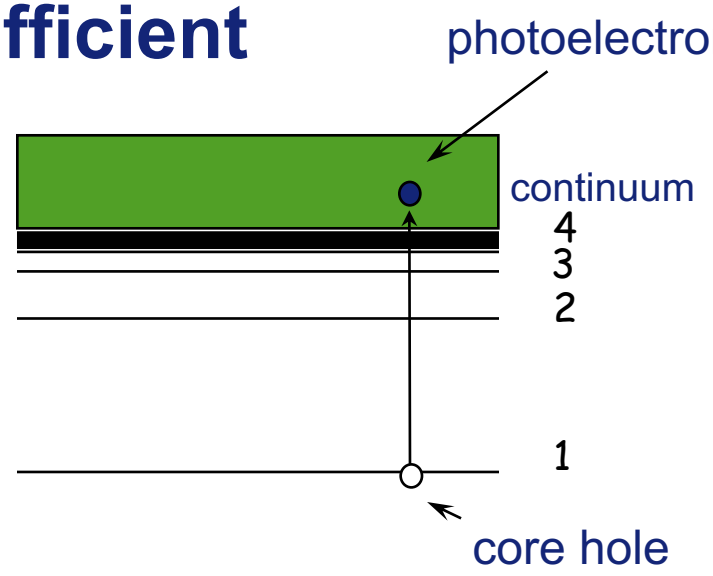

$\langle\psi_i| = \langle 1s|$ $\quad E_i$ $\qquad$ $|\psi_f\rangle = |\varepsilon p\rangle$ $\quad E_f = \hbar\omega + E_i$

$$\mu(\omega) \approx S_0^2 \sum_f \left| \langle \psi_f | \hat{\varepsilon} \cdot \vec{r} | \psi_i \rangle \right|^2$$

Approximations
dipole + single electron + sudden

$\hat{\varepsilon}$: photon polarization $\qquad$ $\vec{r}$: electron position

$|\psi_i\rangle$ relatively easy → ground state of atom; i.e. 1s e^- wavefunction

$|\psi_f\rangle$ very complicated → final state strongly influenced by environment

Isolated atom: atomic absorption coefficient

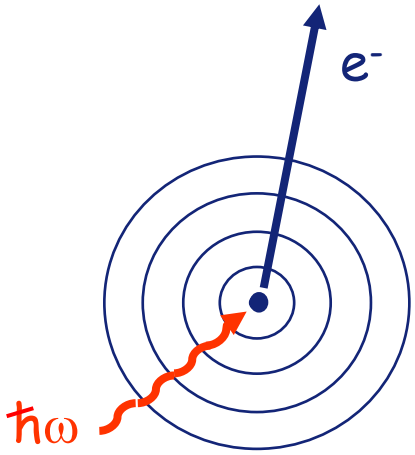

photoelectron free to travel away undisturbed

$$\left|\psi_f\right\rangle = \left|\psi_f^0\right\rangle$$

outgoing spherical wave originating from the absorbing atom

$$\mu_0(\omega) \propto \left|\left\langle \psi_f^0 \right| \hat{\varepsilon}\cdot\vec{r} \left|\psi_i\right\rangle\right|^2$$

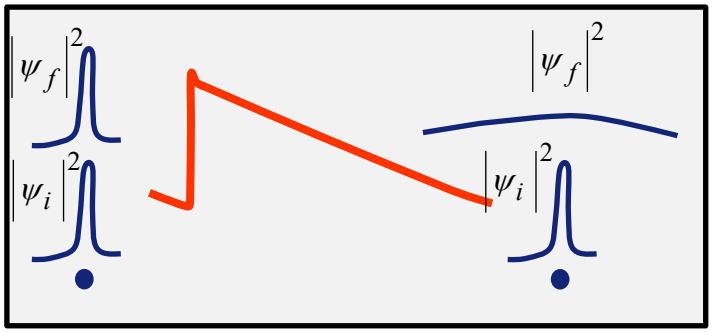

$$\mu_0(\omega) \propto \left|\int d\vec{r}\ \psi_f^0(\vec{r})\ \hat{\varepsilon}\cdot\vec{r}\ \psi_i^*(\vec{r})\right|^2$$

➔ overlap integral of initial and final state wavefunctions: monotonically decreases as function of E

Non-isolated atom

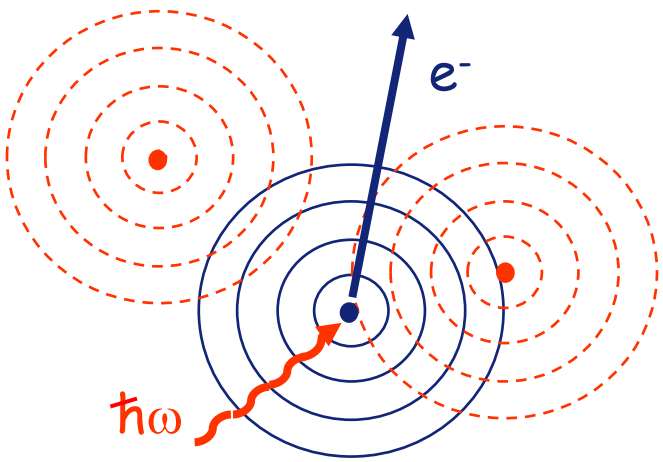

$$|\psi_f\rangle = |\psi_f^0 + \delta\psi_f\rangle$$

sum of the outgoing and all the incoming waves, one per each neighboring atom.

$$\mu(\omega) \propto \left|\langle \psi_f^0 + \delta\psi_f \,|\, \hat{\varepsilon}\cdot\vec{r} \,|\, \psi_i^* \rangle\right|^2$$

$$\mu(\omega) \propto \left| \int d\vec{r}\,[\psi_f^0(\vec{r}) + \delta\psi_f(\vec{r})\,]\,\hat{\varepsilon}\cdot\vec{r}\,\psi_i^*(\vec{r}) \right|^2$$

$$\mu(\omega) \propto \left| \int d\vec{r}\,\psi_f^0(\vec{r})\,\hat{\varepsilon}\cdot\vec{r}\,\psi_i^*(\vec{r}) \right|^2 + 2\,\mathrm{Re}\int d\vec{r}\,\left[\psi_f^{0*}(\vec{r})\,\hat{\varepsilon}\cdot\vec{r}\,\psi_i(\vec{r})\right]\left[\delta\psi_f(\vec{r})\,\hat{\varepsilon}\cdot\vec{r}\,\psi_i^*(\vec{r})\right]$$

$\mu_0(\omega)$

$$+ \left| \int d\vec{r}\,\psi_i^*(\vec{r})\,\hat{\varepsilon}\cdot\vec{r}\,\delta\psi_f(\vec{r}) \right|^2$$

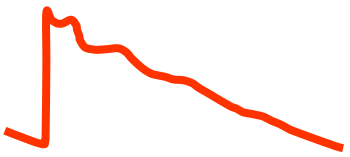

EXAFS

$$(a+ib)+(a-ib)=2a$$

Origin of EXAFS

$$\mu = \mu_0 [\, 1 + \chi \,]$$

χ: fractional change in μ introduced by the neighbors

$$\chi(k) = \frac{2\,\mathrm{Re} \int d\vec{r} \left[\psi_f^{0*}(\vec{r})\, \hat{\varepsilon}\cdot\vec{r}\, \psi_i(\vec{r}) \right] \left[\delta\psi_f(\vec{r})\, \hat{\varepsilon}\cdot\vec{r}\, \psi_i^{*}(\vec{r}) \right]}{\left| \int d\vec{r}\, \psi_f^{0}(\vec{r})\, \hat{\varepsilon}\cdot\vec{r}\, \psi_i^{*}(\vec{r}) \right|^2} \qquad (1)$$

Interference between outgoing wavefunction and backscattered wavelets

Dominant contribution to integral comes from spatial region close to absorber atom nucleus, where the core orbital wavefunction $\psi_i \neq 0$.

The region where $\psi_i \neq 0$ represents simultaneously
the source and the detector for the photoelectron
that probes the local structure around the absorber atom

THE EXAFS EQUATION

To model the EXAFS, we use the EXAFS Equation

$$\chi(k) \sim S_0^2 \, \Sigma_j \, N_j \frac{f_j(k)}{kR_j^{\,2}} \, e^{-2R/\lambda(k)} \, e^{-2k^2\sigma_j^{\,2}} \sin\left[2kR_j + \delta_j(k)\right]$$

where f(k) and δ(k) are photoelectron scattering properties of the neighboring atom.

(the sum is over “shells” of similar neighboring atoms)

If we know f(k) and δ(k), we can determine:

R distance to neighboring atom.
N coordination number of neighboring atom.
σ^2 mean-square disorder of neighbor distance.

The scattering amplitude f(k) and phase-shift δ(k) depend on atomic number *Z* of the scattering atom, so we can also determine the species of the neighboring atom.

10’ Break

The EXAFS equation: simple description

With spherical wave e^{ikr}/kr for the propagating photoelectron, and a scattering atom at a distance r = R, we get:

Region III:
amplitude of backscattering on B

$$\Delta\psi_f \sim \psi^0_f \; \frac{e^{ikR}}{kR} e^{i\delta c} \; |f(k)| \, e^{i\delta s(k)} \; \frac{e^{ikR}}{kR} e^{i\delta c}$$

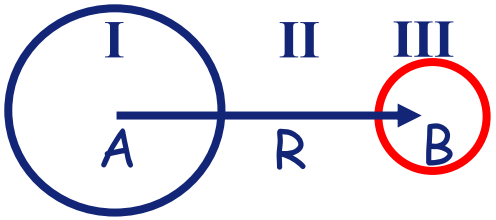

Region I:
amplitude
of outgoing wave

Region II:
amplitude of
wave arriving on B

Region II:
amplitude of ingoing
wave, backscattered from B

where the neighboring atom gives the amplitude $|f(k)|$ and phase-shift $\delta_s(k)$ to the scattered photoelectron.

Substituting into equation (1) and after some math we get (for 1 scattering atom):

$$\chi(k) \sim S_0^2 \frac{f(k)}{kR^2} \sin[2kR + \delta(k)] \qquad \delta(k) = \delta_s(k) + 2\,\delta_c(k)$$

Development of the EXAFS equation

For N scattering atoms, distributed around average distance R with a thermal and static disorder of σ^2 (mean square disorder in R*), we have:

$$\chi(k) \sim S_0^2 \, N \frac{f(k)}{kR^2} \, e^{-2k^2\sigma^2} \sin[2kR + \delta(k)]$$

A real system will have neighboring atoms at different distances and of different types. We add all these contributions to get a version of the EXAFS equation:

$$\chi(k) \sim S_0^2 \, \Sigma_j \, N_j \frac{f_j(k)}{kR_j^{\,2}} \, e^{-2k^2\sigma_j^{\,2}} \sin[2kR_j + \delta_j(k)]$$

To obtain this formula we used a spherical wave for the photoelectron: $\frac{e^{ikr}}{kr}$

* EXAFS takes place on a time scale much shorter than that of atomic motion, so the measurement serves as an instantaneous snapshot of the atomic configuration

The photoelectron mean free path

But the photoelectron can also scatter inelastically*, and may not be able to get back to the absorbing atom. Also: the core-hole has a finite lifetime**, limiting how far the photoelectron can go.

Using a damped wave-function: $\frac{e^{ikr}}{kr} e^{-r/\lambda(k)}$ where λ(k) is the photoelectron's mean free path

(including core hole lifetime), the EXAFS equation becomes:

$$\chi(k) \sim S_0^2 \, \Sigma_j \, N_j \frac{f_j(k)}{kR_j^2} \quad e^{-2Rj/\lambda(k)} \, e^{-2k^2\sigma_j{}^2} \sin \, [2kR_j \, + \, \delta_j(k)]$$

The mean free path λ depends on k.
(for the EXAFS k range, λ ~ 10-20 Å)

The λ and R^{-2} terms make EXAFS a local atomic probe.

* Electrons that have suffered inelastic losses will not have the proper wave vector to contribute to the interference process.

** when the core-hole is filled, it does no longer "detect"

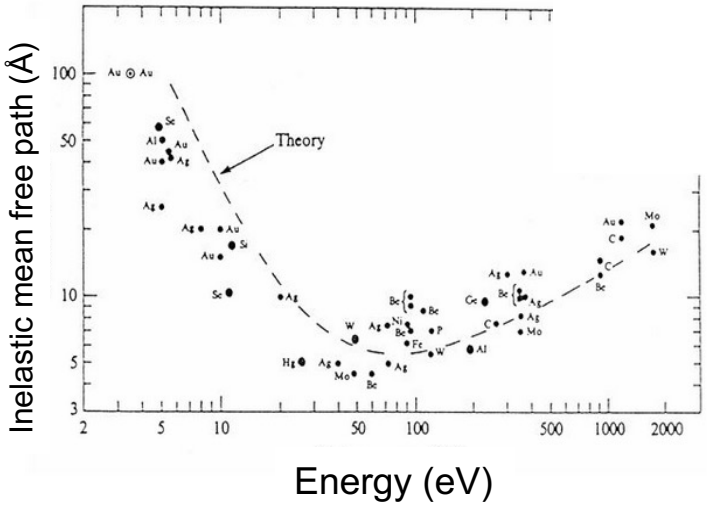

S_0^2 : Amplitude Reduction Term

The amplitude reduction term is due to the relaxation of all the other electrons in the absorbing atom to the hole in the core level:

$$S_0^2 \approx \sum_f \left| \left\langle \Psi_f^{N-1} \mid \Psi_i^{N-1} \right\rangle \right|^2$$

where Ψ_f^{N-1} accounts for the relaxation of the other N-1 electrons relative to these electrons in the unexcited atom: Ψ_0^{N-1} . Typically S_0^2 is taken as a constant:

$$0.7 < S_0^2 < 1.0$$

which is found for a given central atom, and simply multiplies the XAFS χ.

Note that S_0^2 is completely correlated with N.

This, and other experimental and theoretical issues, make EXAFS amplitudes (and therefore N) less precise than EXAFS phases (and therefore R).

Usually S_0^2 is found from a “standard” (data from a sample with well-known structure) and applied to a set of unknowns as a scale factor.

Outline

- EXAFS: a probe of local structure
- EXAFS: simple theoretical description and derivation of EXAFS equation
- XANES: a probe of electronic structure and coordination chemistry
- Applications

X-RAY ABSORPTION FINE STRUCTURE: XANES

K- edge XANES: The example of transition metal oxides

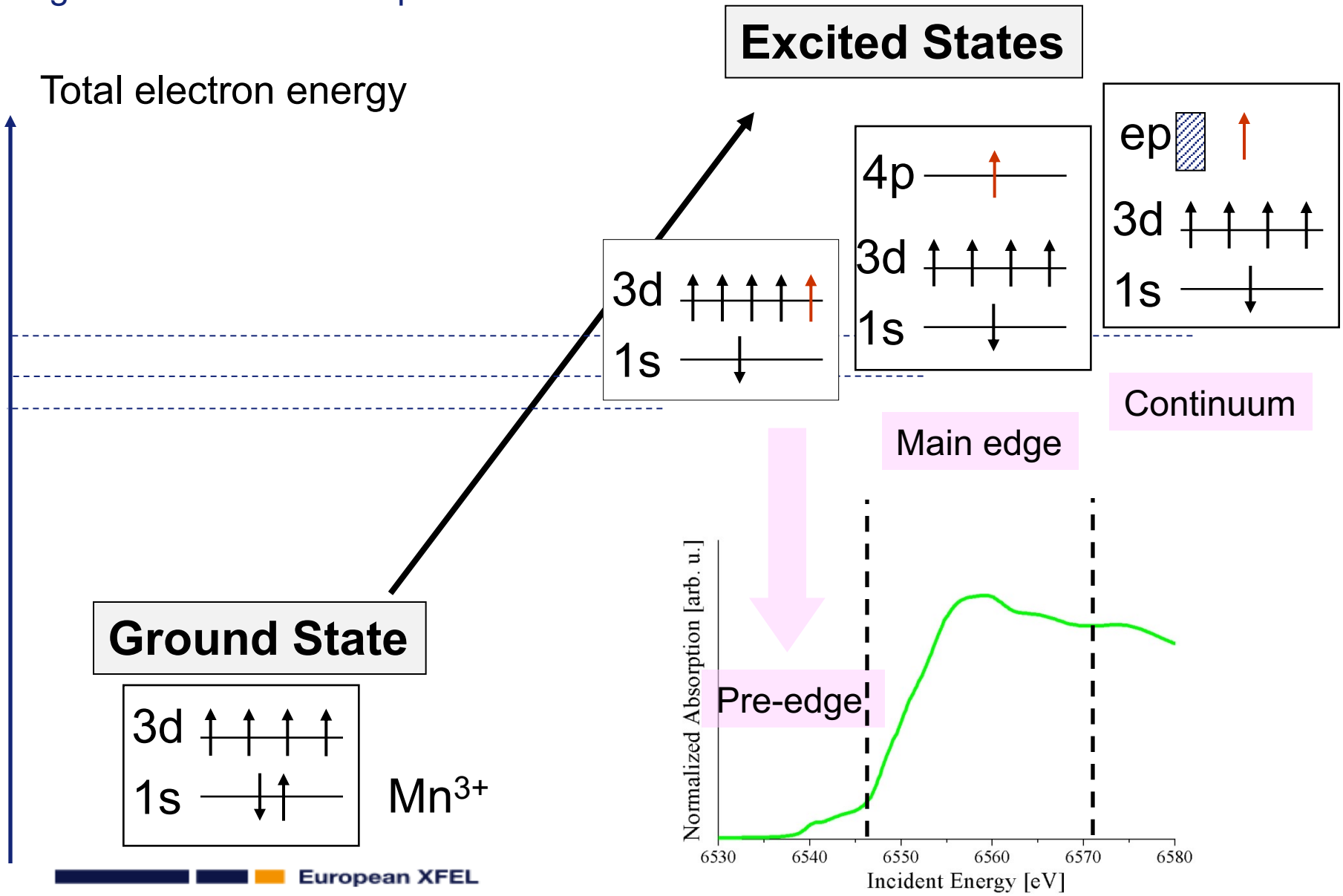

X-RAY ABSORPTION FINE STRUCTURE: XANES

K- edge XANES: chemical shift

Total electron energy

Excited States

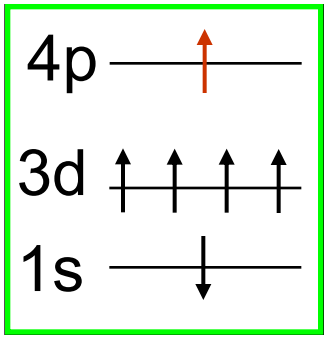

Mn^{3+}

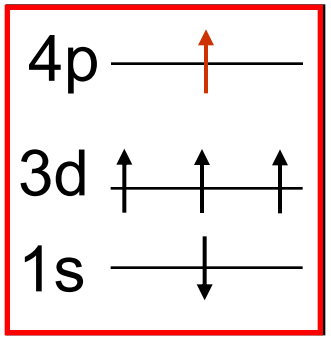

Mn^{4+}

Ground State

Mn^{3+}

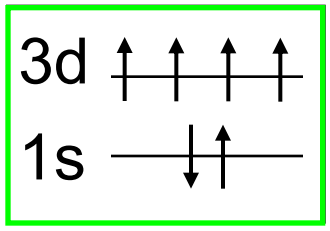

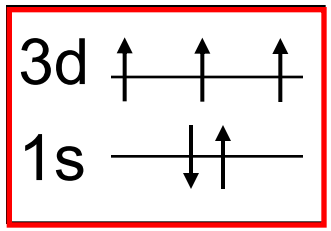

Mn^{4+}

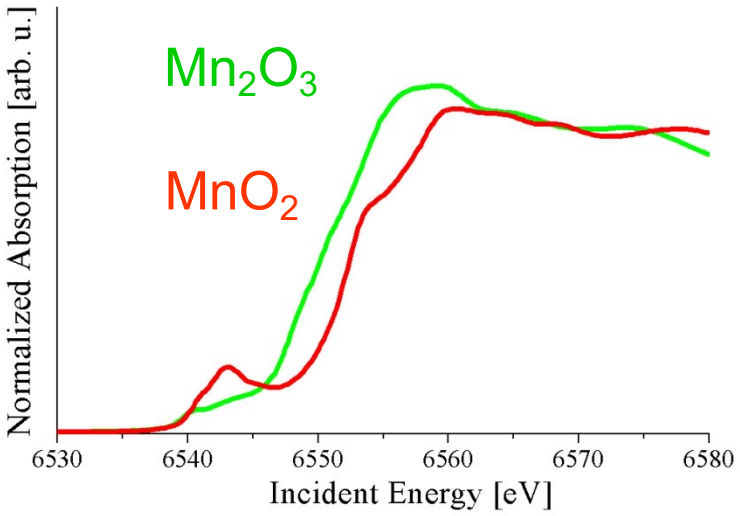

X-RAY ABSORPTION FINE STRUCTURE: XANES

K- edge XANES: pre-edge intensity is linked to coordination

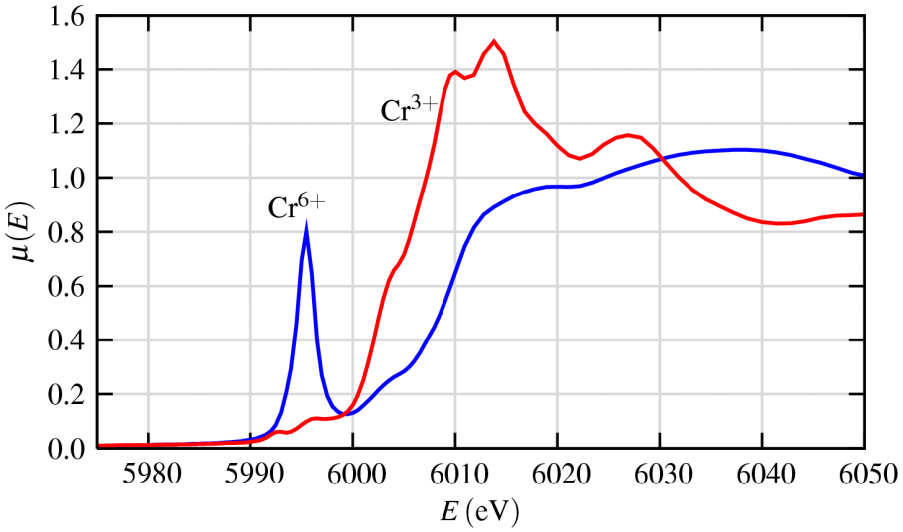

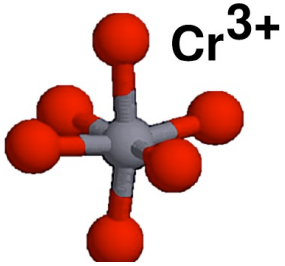

O_h centrosymm
only weak 1s-3d
quadrupole channel

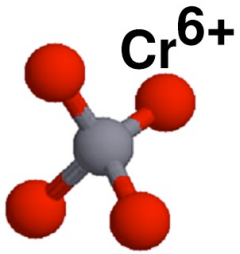

T_d non-centrosymm
4p-3d mixing
1s→ 4p dipole channel

The XANES of Cr^{3+} and Cr^{6+} shows a dramatic dependence on oxidation state and coordination chemistry.

For ions with partially filled d shells, the p-d hybridization changes dramatically as regular octahedra distort, and is very large for tetrahedral coordination.

This gives a dramatic pre-edge peak – absorption to a localized electronic state.

X-RAY ABSORPTION FINE STRUCTURE: XANES

Edge Shifts and Pre-edge Peaks in Fe oxides

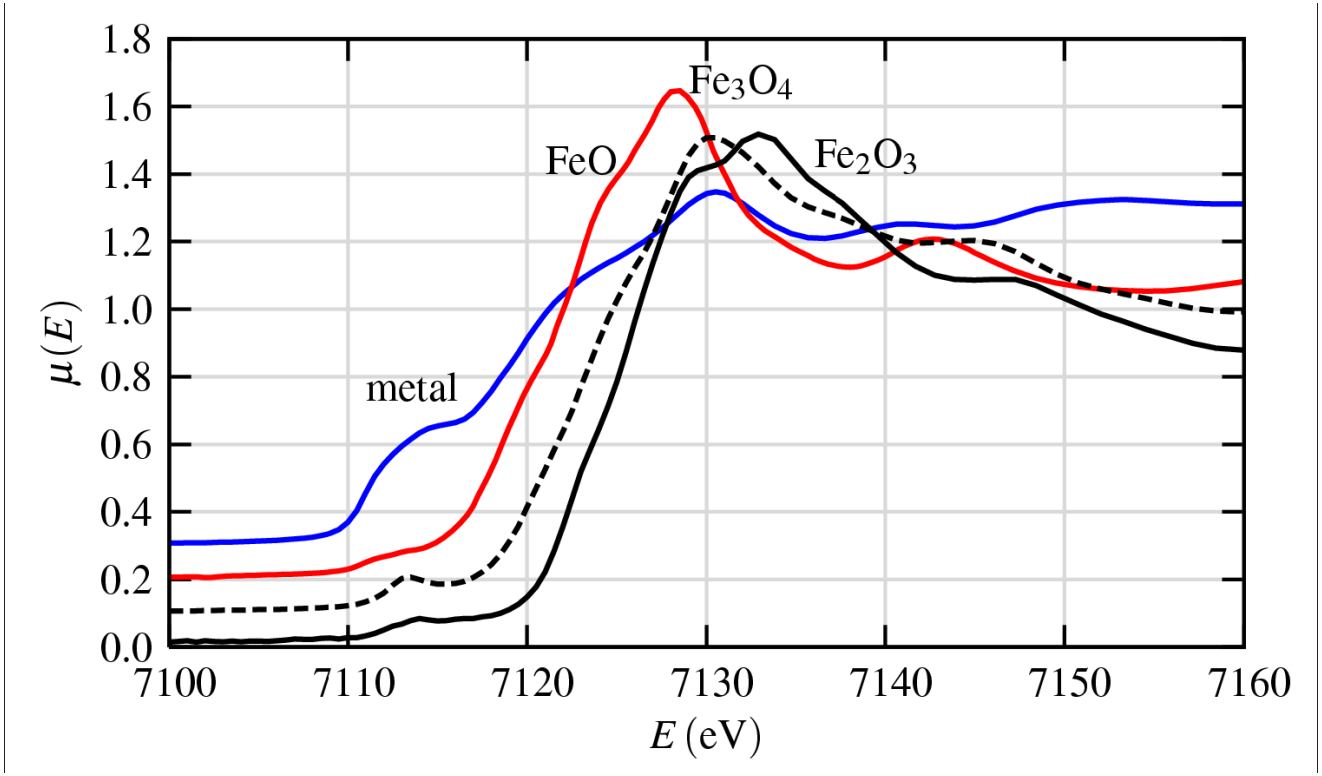

The shift of the edge position can be used to determine the valence state

The heights and positions of pre-edge peaks can also be reliably used todetermine Fe^{3+}/Fe^{2+} ratios (and similar ratios for many cations).

X-RAY ABSORPTION FINE STRUCTURE: XANES

XANES Analysis: Oxidation State

The Normalized XANES from several Fe compounds:

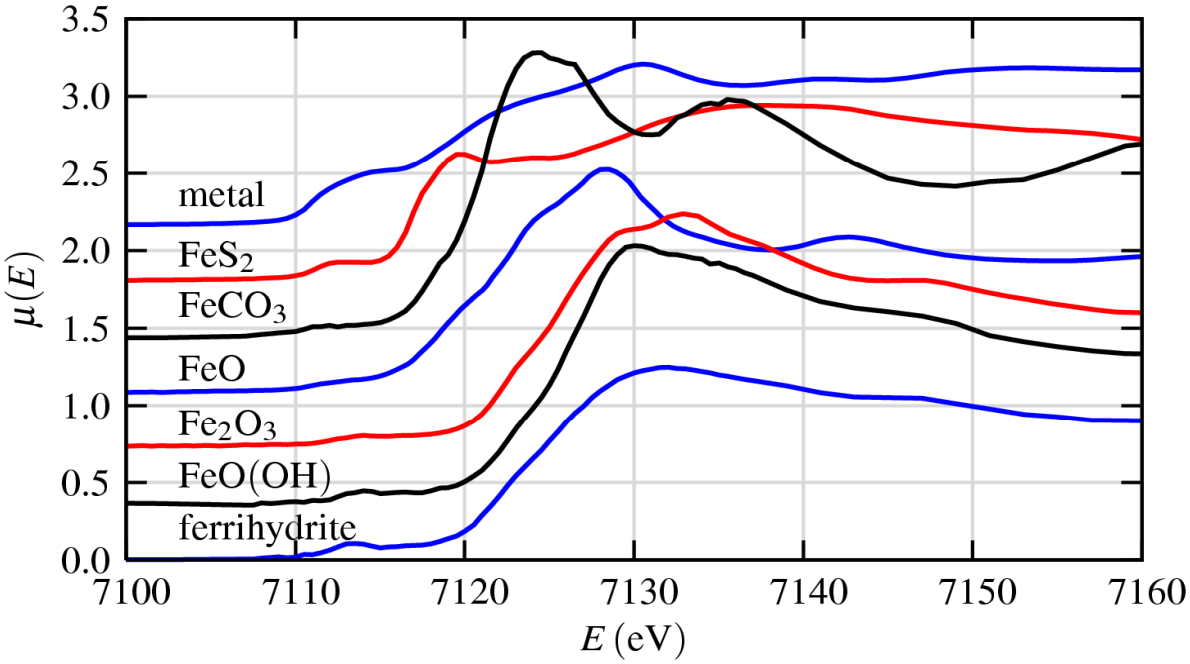

XANES can be used simply as a fingerprint of phases and oxidation state.

XANES analysis can be as simple as making linear combinations of “known” spectra to get compositional fraction of these components.

XANES Interpretation

The EXAFS Equation breaks down at low-k, and the mean-free-path goes up.
This complicates XANES interpretation:

We do not have a simple equation for XANES.

XANES can be described qualitatively (and nearly quantitatively) in terms of

coordination chemistry	regular, distorted octahedral, tetrahedral, . . .
molecular orbitals	p-d orbital hybridization, crystal-field theory, . . .
band-structure	the density of available electronic states
multiple-scattering	multiple bounces of the photoelectron

These chemical and physical interpretations are all related, of course:

What electronic states can the photoelectron fill?

XANES calculations are becoming reasonably accurate and simple. These can help explain what bonding orbitals and/or structural characteristics give rise to certain spectral features.

Quantitative XANES analysis using first-principles calculations are still rare, but becoming possible...

X-RAY ABSORPTION FINE STRUCTURE: XANES

Advances in Theory and Computation

- More robust framework for interpretation of core-hole spectroscopies

1. Multiple Scattering
   - full multiple scattering
   - fully relavistic mono-electronic calculations
   - full potential (non Muffin Tin)
   - *ab initio* Debye-Waller factors
   - improved treatment of inelastic losses

FEFF

FDMNES

crispy 0.2.0

2. Model Hamiltonian (Anderson impurity model)
   - local symmetry as input (crystal field)
   - multiplet calculations (local electronic interactions)

The OCEAN code

3. Many-body perturbation theory
   - detailed interaction between photoelectron and core-hole
   - many body effects such as electronic “self energy” effects, DFT+U
   - optical spectroscopies (UV, visible)
   - partial multiplet effects

XANES: Conclusions

XANES is a much larger signal than EXAFS
XANES can be done at lower concentrations, and less-than-perfect sample conditions.

XANES is easier to crudely interpret than EXAFS
For many systems, the XANES analysis based on linear combinations of known spectra from "model compounds" is sufficient.

XANES is harder to fully interpret than EXAFS
The exact physical and chemical interpretation of all spectral features is still difficult to do accurately, precisely, and reliably.

This situation is improving, so stay tuned to the progress in XANES calculations . . . .

Outline

- EXAFS: a probe of local structure
- EXAFS: simple theoretical description and derivation of EXAFS equation
- XANES: a probe of electronic structure and coordination chemistry
- Applications

XAFS vs Diffraction Methods

❑ Diffraction Methods (X-rays, Neutrons)

- Crystalline materials with long-range ordering -> 3D picture of atomic coordinates
- Materials with only short-range order (amorphous solid, liquid, or solution) -> 1D radial distribution function containing interatomic distances due to all atomic pairs in the sample.

❑ XAFS

- 1D radial distribution function (centered at the absorber)
- Element selectivity
- Higher sensitivity to local distortions (i.e. within the unit cell)
- Charge state sensitivity (XANES)
- Structural information on the environment of each type of atom:
  - distance, number, kind, static and thermal disorder
  - 3-body correlations
- Investigation of matter in the solid (crystalline or amorphous), liquid, solution or gaseous state with same degree of accuracy

XAFS: typical applications

Element selectivity
Electronic structure
Local structure

- Local structure in non-crystalline matter
- Local environment of an atomic impurity in a matrix of different atomic species
- Study of systems whose local properties differ from the average properties
- Detection of very small distortions of local structure

Major historical EXAFS breakthroughs

- Atomic scale structure in solid solutions
- Lattice distortions around impurities in dilute alloys
- Structure of amorphous materials

ATOMIC SCALE STRUCTURE IN SOLID SOLUTIONS

VOLUME 49, NUMBER 19 PHYSICAL REVIEW LETTERS 8 NOVEMBER 1982

Atomic-Scale Structure of Random Solid Solutions: Extended X-Ray-Absorption Fine-Structure Study of $Ga_{1-x}In_xAs$

J. C. Mikkelsen, Jr., and J. B. Boyce
Xerox Palo Alto Research Centers, Palo Alto, California 94304
(Received 23 August 1982)

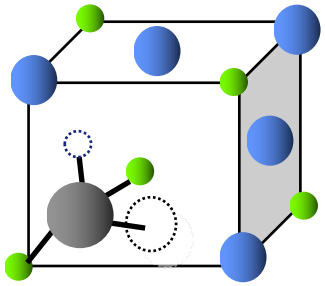

$A_xB_{1-x}C$

- Atomic scale structure not well understood: XRD averages structure over distances that are large on the scale of a lattice constant.
- Calculations of the properties of solid solutions have often relied on simple approximations (i.e. VCA)
- VCA assumes that all atoms occupy average lattice positions defined by X-ray lattice constants

- With the use of the VCA, properties of alloys may be calculated whether or not the alloys's lattice costant varies linearly with composition between those of the end members (follows Vegard's law)

Solid solutions: Vegard's law and the Virtual Crystal Approximation

AC

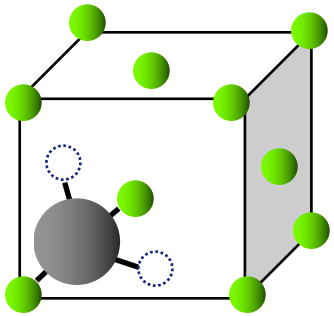

a_{AC}

$$R^0_{AC} = \frac{\sqrt{3}}{4} a_{AC}$$

$AB_x C_{1-x}$

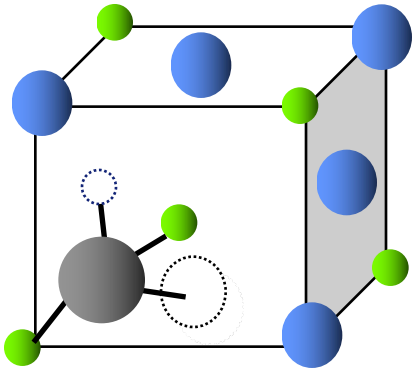

$a(x)$

AB

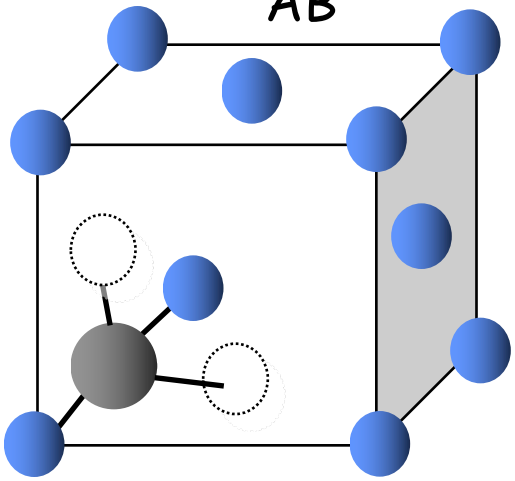

a_{AB}

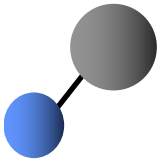

$$R^0_{AB} = \frac{\sqrt{3}}{4} a_{AB}$$

Vegard's Law: $a(x) \approx a_{AC} + (a_{AB} - a_{AC})x$

VCA: $R_{AB}(x) = R_{AC}(x) = \frac{\sqrt{3}}{4} a(x)$

ATOMIC SCALE STRUCTURE IN SOLID SOLUTIONS

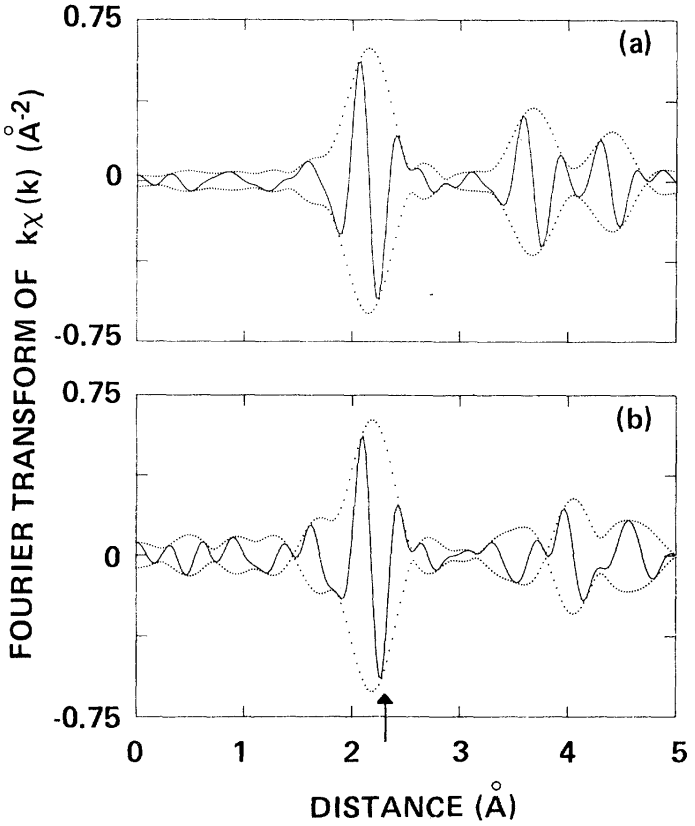

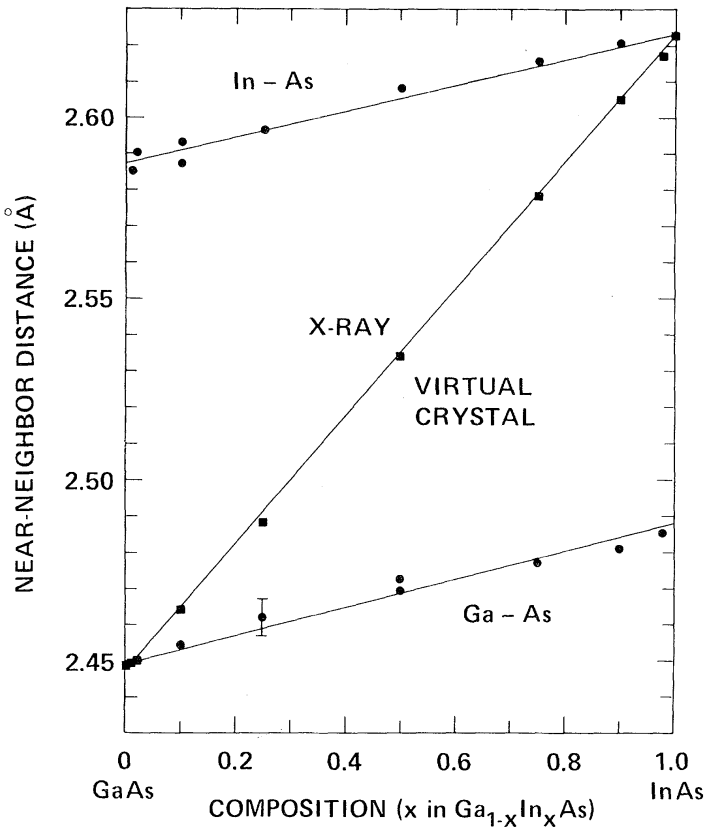

- GaAs and InAs bonds change only by 0.04 Å in whole x range !!
- Contradicts underlying assumptions of VCA
- Important distortions within unit cell accommodated by bond angle distortions

LATTICE DISTORTIONS AROUND IMPURITIES IN DILUTE ALLOYS

PHYSICAL REVIEW B VOLUME 44, NUMBER 18 1 NOVEMBER 1991-II

Lattice distortion of solute atoms in metals studied by x-ray-absorption fine structure

U. Scheuer and B. Lengeler
Institut für Festkörperforschung, Forschungszentrum Jülich, D-5170 Jülich, Germany
(Received 14 February 1991)

- systematic study of substitutional impurities in fcc and bcc metals
- important shifts in first shell bond length detected

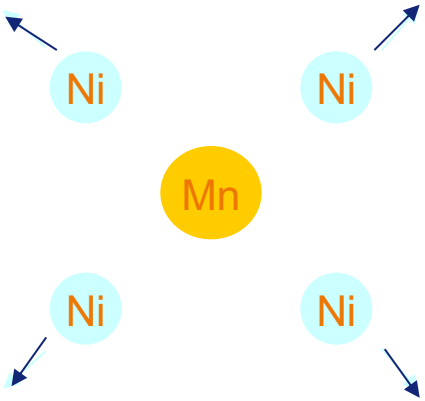

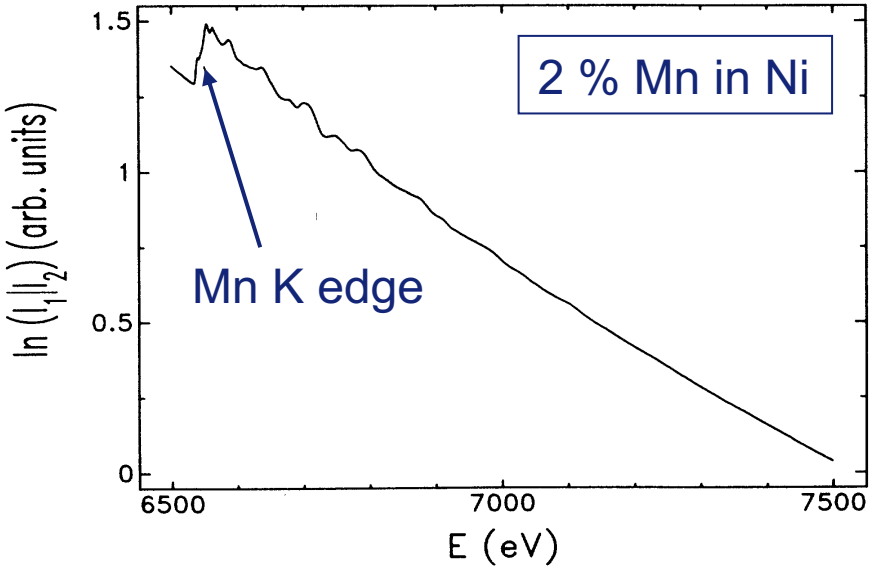

European XFEL

LATTICE DISTORTIONS AROUND IMPURITIES IN DILUTE ALLOYS

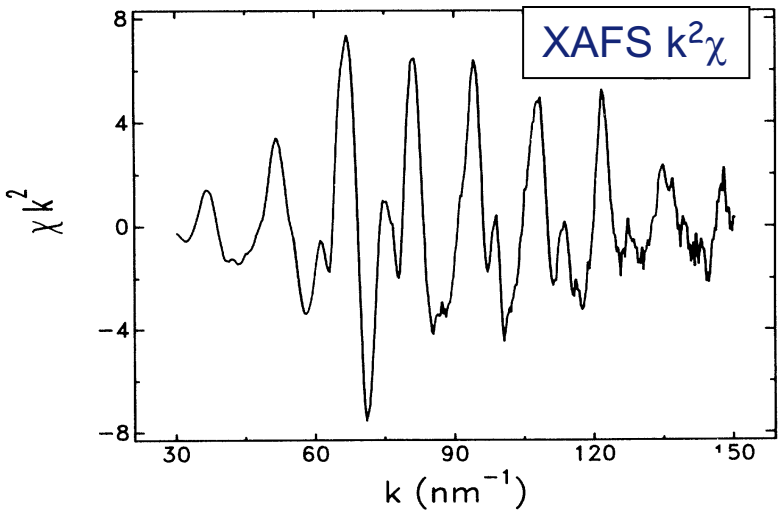

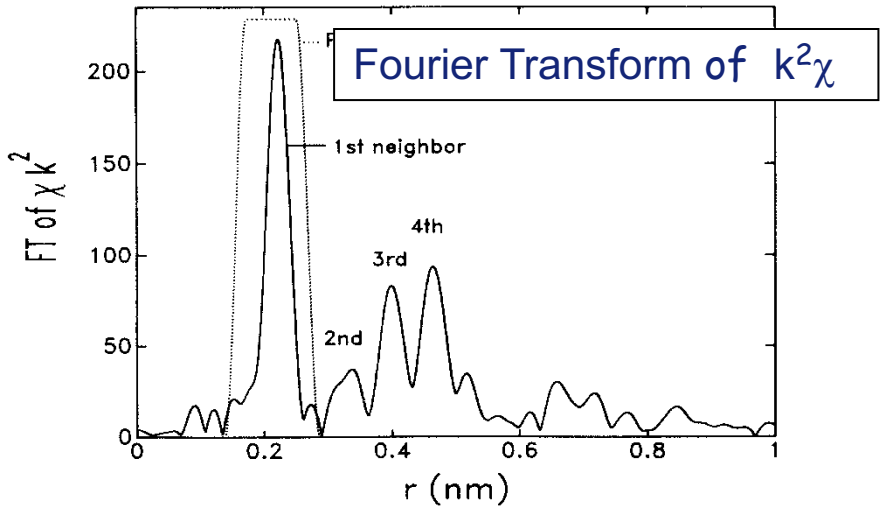

Mn shifts 12 Ni nearest neighbors outwards by:

0.023 ± 0.004 Å

(1 % of distance)

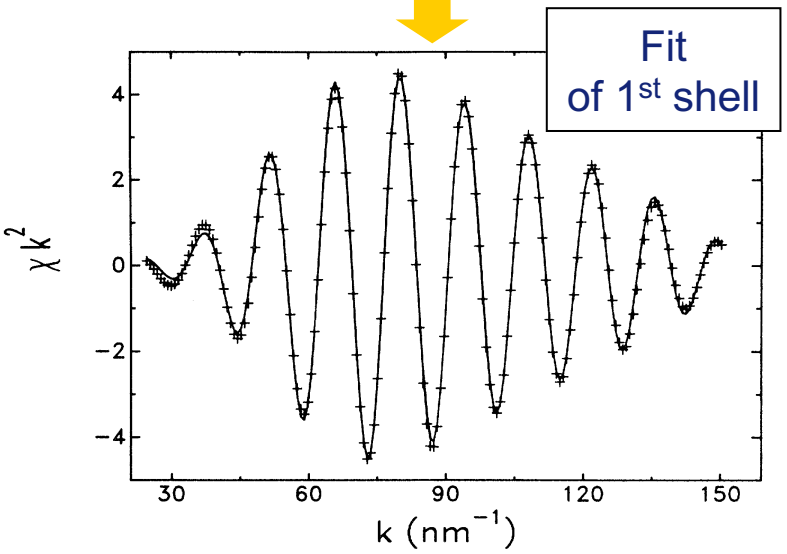

LATTICE DISTORTIONS AROUND IMPURITIES IN DILUTE ALLOYS

Comparison to band structure calculations

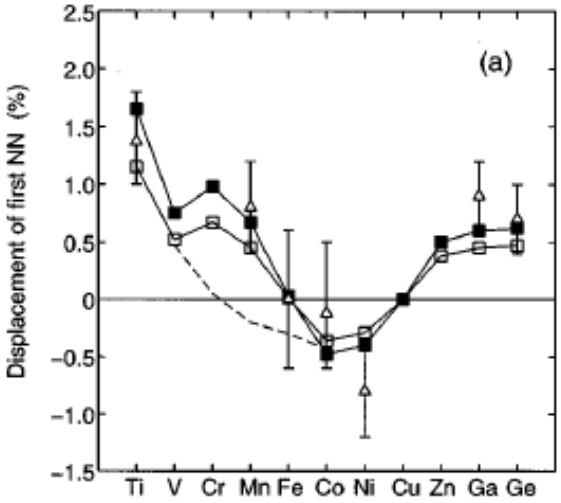

□ ■ Band structure calculations

△ XAS

N. Papanikolau et al., Phys. Rev. B 55, 4157 (1997)

Displacements δ has two contributions:

1. Valence difference between impurity and host

   - change of charge density in impurity cell
   - parabolic dependence $\delta(Z)$

2. Magnetoelastic contribution Cr, Mn, Fe in Cu → majority and minority bands are split

   - large magnetic moment
   - low DOS at Fermi level
   - low binding energy
   - increased interatomic distance

STRUCTURE OF AMORPHOUS MATERIALS

VOLUME 35, NUMBER 9 PHYSICAL REVIEW LETTERS 1 SEPTEMBER 1975

New Method to Measure Structural Disorder: Application to GeO_2 Glass*

D. E. Sayers and E. A. Stern
Physics Department, University of Washington, Seattle, Washington 98195

and

F. W. Lytle
Boeing Company, Seattle, Washington 98124
(Received 24 March 1975)

From X-ray scattering experiments on glasses:

Random network model:
GeO_2 tetrahedra connected by bridging Oxygen with deviations about bond angles such that long range periodicity destroyed

Microcrystalline model:
GeO_2 composed of 15-20 Å crystallites – too small to give rise to sharp diffraction peaks

STRUCTURE OF AMORPHOUS MATERIALS

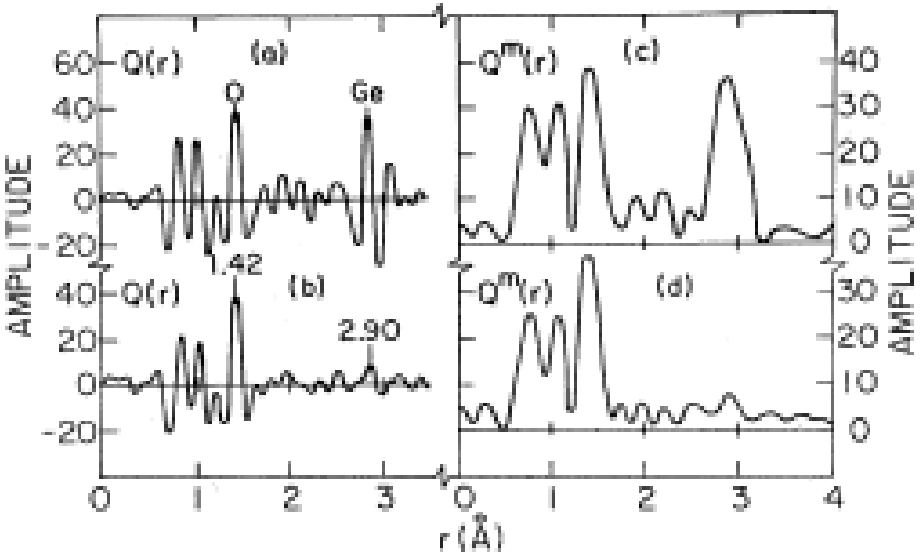

c-GeO_2

g-GeO_2

	r_1	$\Delta\sigma_1$	N_1	r_2	$\Delta\sigma_2$	θ_{Ge-Ge} (deg)
Glass	1.74	0.00 ± 0.018	4.0 ± 0.08	3.15	0.077 ± 0.014	130 ± 6.5
Crystalline (hexagonal)	1.74	···	4	3.15	···	130

EXAFS determines:

- identical 1st shell coordination number (to within 2%)
- increased disorder on Ge-Ge shell

→ microcrystalline model definitively ruled out

SELECTION OF RESULTS

- **Chemistry, Catalysis**
  - Pd redox catalysis: structure, function, reactivity
- **Biology**
  - Ligand discrimination in biological complexes
- **Environmental Science**
  - As sequestration by organic sulphur in peat
- **Matter at Extreme Conditions**
  - Chemistry of Xe at extreme conditions

PD REDOX CATALYSIS: STRUCTURE – FUNCTION – REACTIVITY

ID24, ESRF

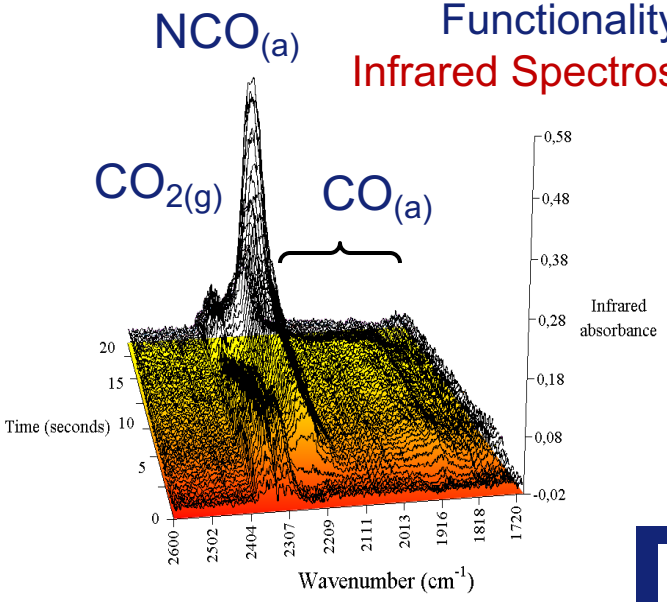

Functionality
Infrared Spectroscopy

Structure
EXAFS

Reactivity
Mass Spectrometry

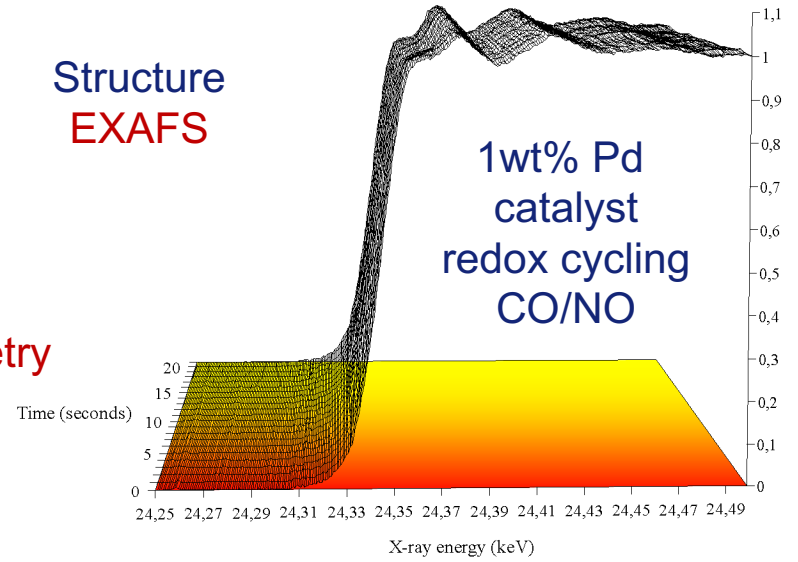

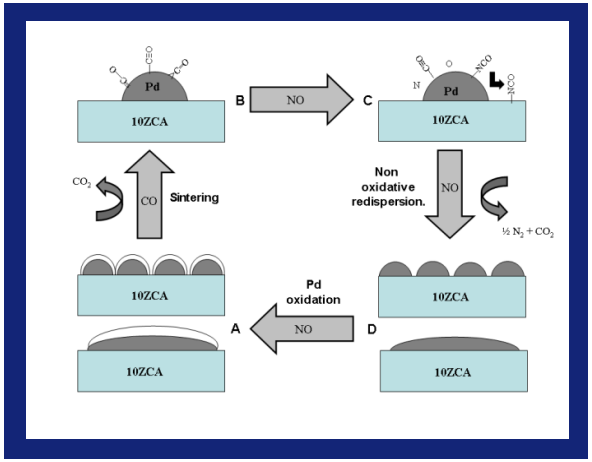

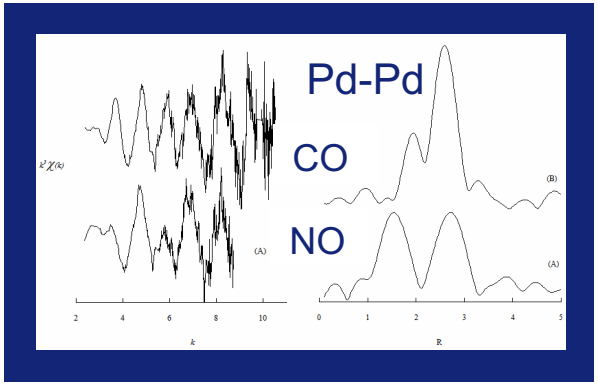

- Pd particles are not passive entities
- Evidence of fast morphological change

MA Newton et al., Nature Materials (2007)

Full quantitative multiple scattering analysis of XAS: Application to $K_3Fe(CN)_6$ and $K_4Fe(CN)_6$

- Example of application of MXAN -

$K_3Fe(CN)_6$

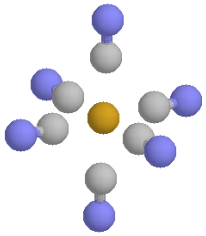

- Fitting procedures now possible also in XANES region
- Higher sensitivity to geometry and chemical nature of scattering atoms
- For biological systems, EXAFS not very sensitive to number and chemical nature of ligands

➢ **Combined quantitative multiple scattering analysis of EXAFS and XANES**

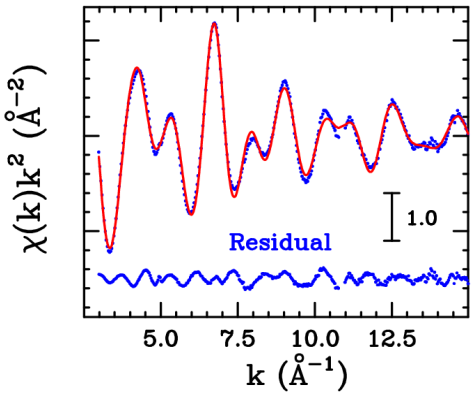

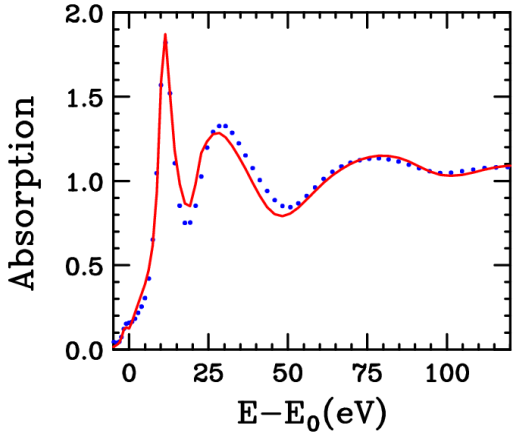

K. Hayakawa et al., J. Am. Chem. Soc. 126, 15618 (2004)

BM29, ESRF

LIGAND DISCRIMINATION IN ORGANIC COMPLEXES

- Quantitative analysis using CN, CO and NO as ligands

  EXAFS: cannot discriminate (residuals within 3%)

  XANES: can discriminate CN, CO or NO

Table 2. Structural Parameters for Fe^{3+} Complexes Obtained from the MXAN Data Analysis

	CN	CO	NO
R_{Fe-L_1} (Å)	1.93(1)	1.94(1)	1.92(1)
$R_{L_1-L_2}$ (Å)	1.15(1)	1.11(1)	1.16(1)
$\theta_{Fe-L_1-L_2}$ (deg)	180(1.3)	180[a]	180[a]
R_{sq}	20.8	28.8	50.0

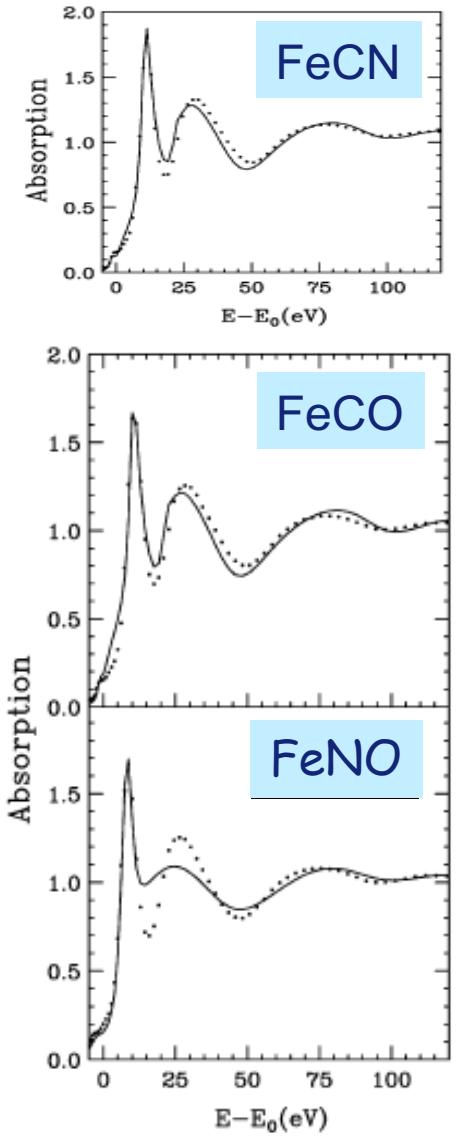

BM29, ESRF

- **First quantitative demonstration of the ability of XANES in ligand discrimination for both first and second shell coordinating atoms**.

ARSENIC SEQUESTRATION BY ORGANIC SULPHUR IN PEAT

Wetlands cover more than 6% of the global ice-free land area

Play major role in storage, transformation, mobilization of trace elements

Sorption of As to peat thought to suppress As mobility, but binding mechanisms unknown

Does natural organic matter serve as geochemical trap for As ?

As K- EXAFS (3-1000 ppm)

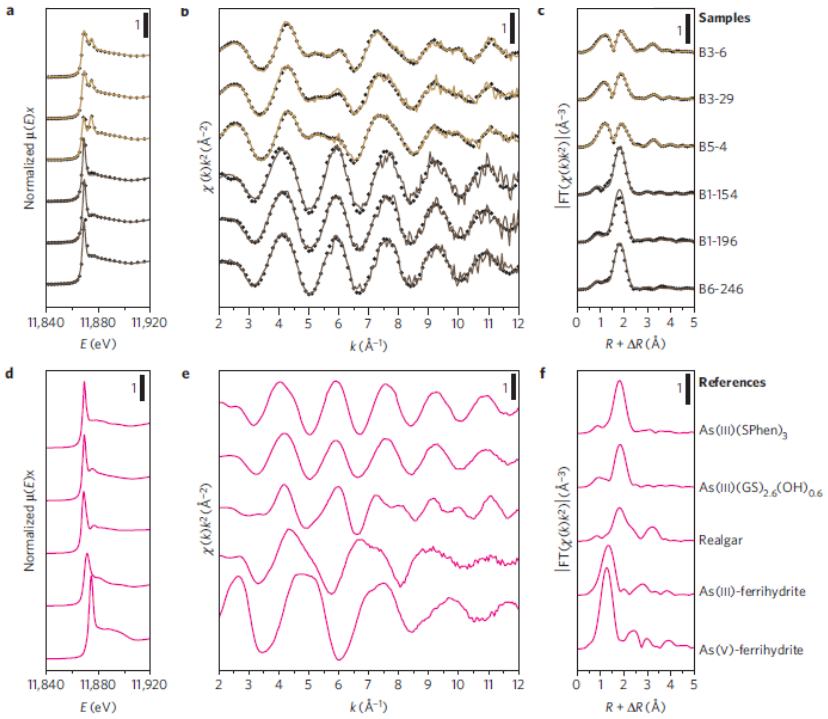

Trap: covalent bonds between As^{+3} and organic S groups

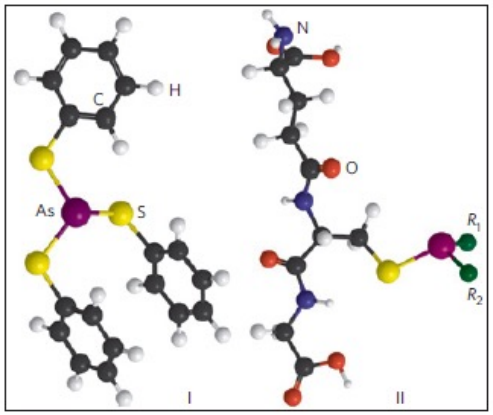

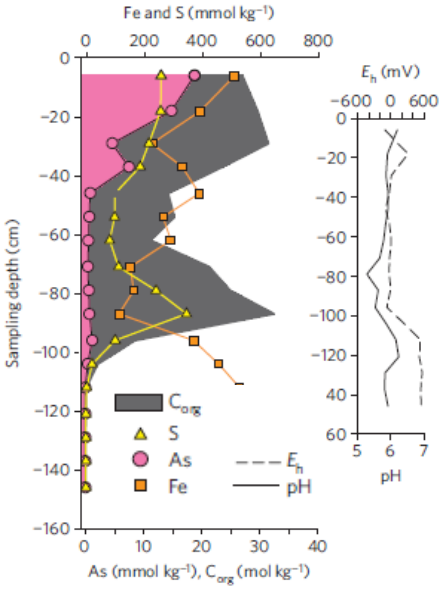

1. Spectroscopic evidence for As binding to peat
2. Identified dominating binding mechanism
3. Quantified extent of As binding to peat

Langner Nature Geoscience 2012

BM23, ESRF

CHEMISTRY OF XENON AT EXTREME CONDITIONS

Understand abundance of Xe in atmospheres of giant planets
Deficiency in Earth and Mars atmospheres

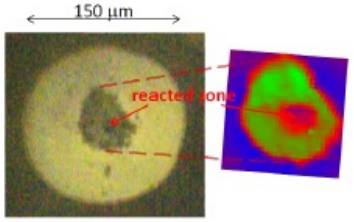

BM23, ESRF

Xe [Kr] 4d10 5s2 5p6

- *"Rare gases reluctant to form bonds"*
- Xe oxides not stable at ambient P, T
- Xe-O interactions at HP

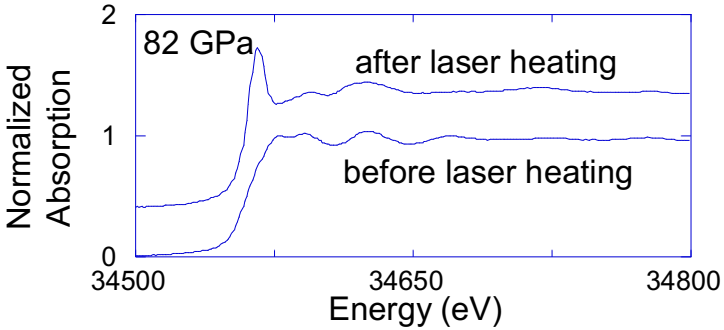

nature chemistry AR
PUBLISHED ONLINE: 11 NOVEMBER 2012 | DOI: 10.10

Stability of xenon oxides at high pressures

None of the predicted phases observed
XRD alone unable to determine oxide structure

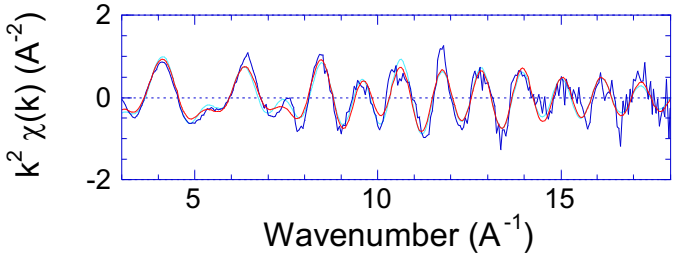

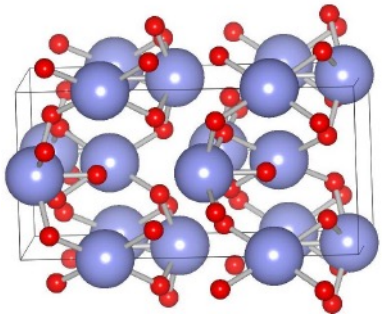

Xe_2O_5
P4/ncc space group

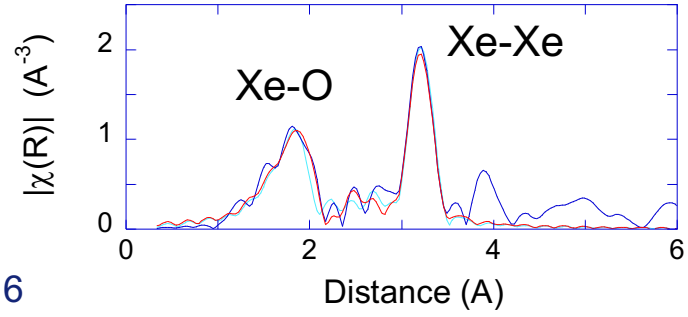

Dewaele Nature Chemistry 2016

MORE INFORMATION: ON THE INTERNET

International XAFS Society: http://ixs.iit.edu/

Tutorials and other Training Material: http://xafs.org/Tutorials

→ http://gbxafs.iit.edu/training/tutorials.html

Software Resources EXAFS:

http://xafs.org/Software

http://leonardo.phys.washington.edu/feff

http://gnxas.unicam.it/

MORE INFORMATION: BOOKS AND REVIEW ARTICLES

Fundamentals of XAFS

Introduction to XAFS: A Practical Guide to X-ray Absorption Fine Structure Spectroscopy,
G. Bunker, Cambridge University Press, 2010

Recent Review XAS XES:

X-Ray Absorption and X-Ray Emission Spectroscopy: Theory and Applications

Editor(s): Jeroen A. Van Bokhoven, Carlo Lamberti
Published Online: 22 JAN 2016 09:48PM EST
DOI: 10.1002/9781118844243

FEFF

Theoretical approaches to x-ray absorption fine structure
J. Rehr et al., Rev. Mod. Phys. 72, 621 - 654 (2000)

Ab initio theory and calculations of X-ray spectra, J.J. Rehr, J.J. Kas, M.P. Prange, A.P. Sorini, Y. Takimoto, F.D. Vila, Comptes Rendus Physique 10 (6) 548-559 (2009).

Parameter-free calculations of x-ray spectra with FEFF9, J.J. Rehr, J.J. Kas, F.D. Vila, M.P. Prange, K. Jorissen, Phys. Chem. Chem. Phys., 12, 5503-5513 (2010).

GNXAS

X-ray absorption spectroscopy and n-body distribution functions in condensed matter (I): theory of the GNXAS data-analysis method
A. Filipponi, A. Di Cicco and C. R. Natoli, Phys. Rev. B 52, 15122 (1995)

MXAN

Geometrical fitting of experimental XANES spectra by a full multiple-scattering procedure
M. Benfatto and S. Della Longa J. Synchr. Rad. 8, 1087 (2001)

Progresses in the MXAN Fitting Procedure
K. Hayakawa, K. Hatada, S. Dell Longa, P. D'Angelo and M. Benfatto, AIP Conf. Proc. 882, 111-113 (2007).

How to calculate μ

energy density *u* carried by X-ray beam is:

$$u = \frac{\varepsilon_o E_0^2}{2} = \frac{\varepsilon_o \omega^2 A_0^2}{2}$$

linear absorption coefficient μ measures the **energy density reduction** due to the interaction with the system of atoms:

$$\mu(\omega) = -\frac{1}{u}\frac{du}{dx}$$

$$\mu(\omega) = -\frac{2}{\varepsilon_0 \omega^2 A_0^2}\frac{du}{dx}$$

$$\mu(\omega) = -\frac{2}{\varepsilon_0 \omega^2 A_0^2}\frac{d}{dx}\left[\hbar\omega\, n_{ph}\right]$$

$$\mu(\omega) = -\frac{2\hbar}{\varepsilon_0 \omega A_0^2}\frac{d}{dx}\left[\, n_{ph}\right]$$

$$\mu(\omega) = \frac{2\hbar}{\varepsilon_0 \omega A_0^2}\, n \sum_f W_{if}$$

n = atomic density

W_{if} = transition probability

X-ray Absorption

I. Lets consider the interaction between:

Monochromatic X-ray beam ($\omega = 2\pi\nu$) + **monoatomic sample**

EM field (classic) + atom (quantistic)

(semi-classical description)

II. $\mu \sim \mu_{\text{photoelectric absorption}}$ for $1 < E < 50$ keV

III. Qualitatively, interaction process is:

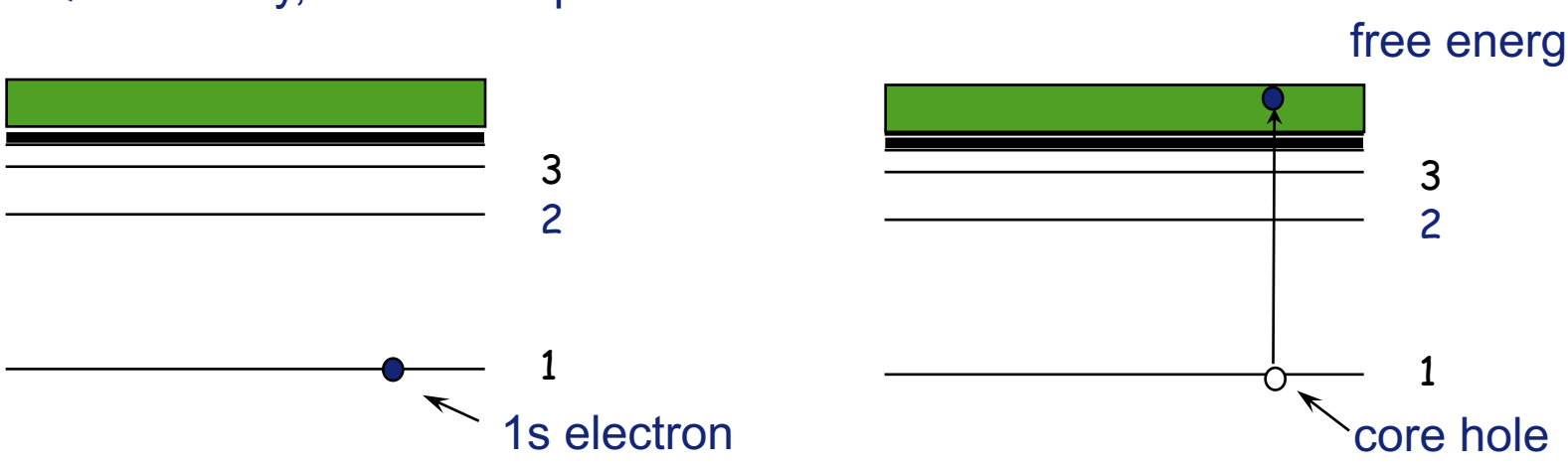

$| \Psi_i >$, E_i $| \Psi_f >$, $E_f = E_i + \hbar\omega$

Transition probability: Golden Rule

- **μ(ω) depends on:**
  - atomic density n
  - transition probability W_{if} of atom from $|\Psi_i\rangle$ to $|\Psi_f\rangle$

$$\mu(\omega) = \frac{2\hbar}{\varepsilon_0 \omega A_0^2} n \sum_f W_{if} \qquad (1)$$

- **time-dependent perturbation theory** (power series of EM field - atom interaction potential)
- The interaction is in general **WEAK:** can limit series to 1st order: **Golden Rule**

$$W_{if} = \frac{2\pi}{\hbar} \left| \langle \Psi_f | \hat{H}_I | \Psi_i \rangle \right|^2 \rho(E_f) \qquad (2)$$

$\hat{H}_I$ EM field - atom interaction hamiltonian operator

$\left| \langle \Psi_f | \hat{H}_I | \Psi_i \rangle \right|$ Matrix element of H_I between initial and final state

$\rho(E_f)$ Density of final states, compatible with energy conservation: $E_f = E_i + \hbar\omega$

APPENDIX 1

- the interaction hamiltonian for photoelectric absorption (see Appendix 1) is (to 1st order):

$$\hat{H}_I = i\hbar \frac{e}{m} \sum_j \vec{A}(\vec{r}_j) \cdot \vec{\nabla}_j \qquad (3) \qquad \vec{A}(\vec{r}_j) = |A_0| \, \hat{\varepsilon} \, e^{i\vec{k}\cdot\vec{r}_j}$$

- the transition probability for photoelectric absorption of a monochromatic, polarized and collimated photon beam is [(3) into (2)]:

$$W_{if} = \frac{\pi\hbar e^2}{m^2} |A_0|^2 \left| \left\langle \Psi_f \left| \sum_j e^{i\vec{k}\cdot\vec{r}_j} \, \hat{\varepsilon} \cdot \vec{\nabla}_j \right| \Psi_i \right\rangle \right|^2 \rho(E_f) \qquad (4)$$

$$W_{if} = \frac{\pi\hbar e^2}{m^2} |A_0|^2 \left| \left\langle \Psi_f \left| \sum_j e^{i\vec{k}\cdot\vec{r}_j} \, \hat{\varepsilon} \cdot \vec{\nabla}_j \right| \Psi_i \right\rangle \right|^2 \rho(E_f)$$

Dipole approximation

- further simplification:

$$e^{i\vec{k}\cdot\vec{r}_j} = 1 + i\,\vec{k}\cdot\vec{r}_j - \frac{\left(\vec{k}\cdot\vec{r}_j\right)^2}{2!} \ldots \cong 1 \quad if \quad \left|\vec{k}\cdot\vec{r}_j\right|^2 << 1$$

- transition probability in dipole approximation:

$$W_{if} = \frac{\pi\,\hbar\,e^2}{m^2}\,\left|A_0\right|^2\,\left|\left\langle\Psi_f\left|\sum_j \hat{\varepsilon}\cdot\vec{\nabla}_j\right|\Psi_i\right\rangle\right|^2\,\rho\left(E_f\right)$$

- alternative and equivalent expression (see Appendix 2):

$$W_{if} = \frac{\pi e^2\omega^2}{\hbar}\,\left|A_0\right|^2\,\left|\left\langle\Psi_f\left|\sum_j \hat{\varepsilon}\cdot\vec{r}_j\right|\Psi_i\right\rangle\right|^2\,\rho\left(E_f\right) \qquad (5)$$

- finally one gets [(5) into (1)]:

$$\mu(\omega) = \frac{2\,\pi\,e^2\,\omega}{\varepsilon_0}\,n\left|\left\langle\Psi_f\left|\sum_j \hat{\varepsilon}\cdot\vec{r}_j\right|\Psi_i\right\rangle\right|^2\,\rho\left(E_f\right) \qquad (6)$$

APPENDIX 1

$$\mu(\omega) = \frac{2\pi e^2 \omega}{\varepsilon_0} n \sum_f \left| \left\langle \Psi_f \left| \sum_j \hat{\varepsilon} \cdot \vec{r}_j \right| \Psi_i \right\rangle \right|^2 \rho(E_f)$$

- if $|\Psi_i>$ and $|\Psi_f>$ are known (if wavefunctions and energies can be calculated):

  1) calculate W_{if}
  2) calculate $\mu(\omega)$

- in practice, one is interested in inverse process:

  1) measure $\mu(\omega)$
  2) extract EXAFS
  3) obtain information on local structure through $|\Psi_f>$

- but, to obtain structural info, one still needs to calculate $|\Psi_i>$ and $|\Psi_f>$ or at least be able to express their structural properties in parametric form

$|\Psi_i>$ relatively easy → ground state of atom

$|\Psi_f>$ in general very complicated → in principle, all electrons are involved (multi body process, final state strongly influenced by environment)

Single electron approximation

- large part of μ due to elastic transitions:
  - only 1 electron out of N modifies its state: leaves its deep core level
  - all other N-1 "passive" electrons relax their orbitals to adapt to the new potential created by presence of core hole

- remaining part of μ due to inelastic transitions:
  - primary excitation of core electron provokes successive excitations of other (external) electrons (shake up, shake off processes)
  - excess energy distributed among all excited electrons

$$\mu(\omega) = \mu_{el}(\omega) + \mu_{inel}(\omega)$$

where $$\mu_{el}(\omega) \propto \left| \left\langle \Psi_f^{N-1} \psi_f \right| \hat{\varepsilon} \cdot \vec{r} \left| \Psi_i^{N-1} \psi_i \right\rangle \right|^2 \rho(\varepsilon_f)$$

Ψ_i^{N-1} Slater determinant of "passive" electrons' wavefunctions

ψ, r, ε_f Wavefunction, position vector, final energy of "active" electron

"Sudden" approximation and overlap factor

If photoelectron energy is sufficiently high (E > few 10 eV above edge)

- time to exit atom << relaxation time of passive electrons
- its state not influenced by passive electrons relaxation

$$\mu_{el}(\omega) \propto S_0^2 \left| \langle \psi_f | \hat{\varepsilon} \cdot \vec{r} | \psi_i \rangle \right|^2 \rho(\varepsilon_f) \qquad (7)$$

where $$S_0^2 = \left| \left\langle \Psi_f^{N-1} \middle| \Psi_i^{N-1} \right\rangle \right|^2$$ (S_0^2 ~ 0.7 – 1.0)

→ **Allows to reduce interpretation of EXAFS to the calculation of the final state of ONLY the photoelectron**

APPENDIX 1

$$\mu(\omega) \approx \sum_f \left| \langle \psi_i | \hat{\varepsilon} \cdot \vec{r} | \psi_f \rangle \right|^2$$

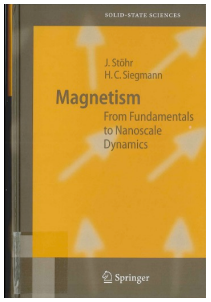

dipole operator

$$P_\alpha^q = \boldsymbol{\epsilon} \cdot \mathbf{r} = \boldsymbol{\epsilon}_\alpha^q \cdot \mathbf{r}$$

α = x, y , z X-ray prop direction

q = +1, 0, -1 polarization states

(q$\hbar$ photon angular momentum)

electron position vector $\mathbf{r} = x\mathbf{e}_x + y\mathbf{e}_y + z\mathbf{e}_z$

photon polarization vectors

$$\epsilon_x^0 = \epsilon_x = e_x \qquad \epsilon_y^0 = \epsilon_y = e_y \qquad \epsilon_z^0 = \epsilon_z = e_z$$

linear polarization

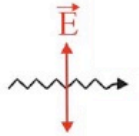

$$\epsilon_z^\pm = \mp \frac{1}{\sqrt{2}} (\epsilon_x \pm \mathrm{i}\, \epsilon_y)$$

circular polarization with **k** // z

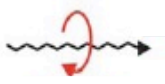

dipole operator in terms of spherical harmonics

$$P_z^\pm = \boldsymbol{\epsilon}_z^\pm \cdot \mathbf{r} = \mp \frac{1}{\sqrt{2}} (x \pm \mathrm{i}y) = r \sqrt{\frac{4\pi}{3}}\, Y_{1,\pm 1}$$

$$P_z^0 = \boldsymbol{\epsilon}_z \cdot \mathbf{r} = \qquad z \qquad = r \sqrt{\frac{4\pi}{3}}\, Y_{1,0}.$$

APPENDIX 1

$$\mu(\omega) \approx \sum_f \left| \left\langle \psi_f \left| \hat{\varepsilon} \cdot \vec{r} \right| \psi_i \right\rangle \right|^2$$

$$\underbrace{\delta(m_s', m_s)}_{\text{spin}} \underbrace{\langle R_{n',l}(r)|r|R_{n,c}(r)\rangle}_{\text{radial}} \underbrace{\sum_{m_c, m_l, p} e^q_{\alpha,p} \langle l, m_l | C^{(1)}_p | c, m_c \rangle,}_{\text{angular}}$$

matrix elements factor into spin, radial and angular parts

By looking at the non-zero matrix elements we get the dipole selection rules

$$\begin{aligned}
&\Delta l = l' - l = \pm 1, \\
&\Delta m_l = m_l' - m_l = q = 0, \pm 1, \\
&\Delta s = s' - s = 0, \\
&\Delta m_s = m_s' - m_s = 0.
\end{aligned}$$

where $q\hbar$ is the X-ray angular momentum

Interaction Hamiltonian

- EM field (E, B) described by Coulomb Gauge:

$$\nabla \cdot A = 0$$

$A(r,t)$: $A_{\gamma}(r,t) \circlearrowleft 0$, $A_{//}(r,t) = 0$

- Atom described by charged particles α:

m_α , q_α

r_α, p_α --> $\frac{h}{i}\nabla_\alpha$

- Total Hamiltonian:

$$H = \sum_\alpha \frac{1}{2m_\alpha}\left[p_\alpha - q_\alpha A(r_\alpha)\right]^2 - \sum_\alpha \frac{g_\alpha q_\alpha}{m_\alpha} S_\alpha \cdot B(r_\alpha) + V_{Coul} + H_{rad}$$

(1) (2) (3) (4)

Total Hamiltonian: Terms

(1) Kinetic energy

$$\sum_{\alpha} \frac{1}{2m_\alpha} \left[p_\alpha - q_\alpha A(r_\alpha)\right]^2 = \sum_{\alpha} \frac{1}{2} m_\alpha \dot{r}_\alpha^2$$

$$\dot{r}_\alpha = \frac{1}{ih}\left[r_\alpha, H\right] = \frac{\partial H}{\partial p_\alpha} = \frac{1}{m_\alpha}\left[p_\alpha - q_\alpha A(r_\alpha)\right]$$

(2) Magnetic term

$$\sum_{\alpha} \frac{g_\alpha q_\alpha}{m_\alpha} S_\alpha \cdot B(r_\alpha)$$

(3) Coulomb energy between pairs of charged particles V_{Coul}

(4) Transverse field energy density H_{rad}

Interaction Terms

$$H = H_0 + H_I = H_{particles} + H_{Rad} + H_I$$

$$H_0 = H_{particles} + H_{rad} = \sum_\alpha \frac{p_\alpha^2}{2m_\alpha} + V_{Coul} + H_{rad}$$

well defined eigenstates valid for atoms, molecules, solids

$$H_I = -\sum_\alpha \left[\frac{q_\alpha}{m_\alpha} p_\alpha \, A(r_\alpha)\right] - \sum_\alpha \left[\frac{g_\alpha q_\alpha}{m_\alpha} S_\alpha \, B(r_\alpha)\right] + \sum_\alpha \left[\frac{q_\alpha^2}{2m_\alpha} A^2(r_\alpha)\right]$$

H_{I1} $\qquad$ H_{I2}^{spin} $\qquad$ H_{I2}

linear in A: photon creation or absorption

quadratic in A: scattering (one photon in, one photon out)

Orders of Magnitude

$$\frac{H_{I2}}{H_{I1}} = \frac{\frac{q^2 A^2}{m}}{\frac{q\ A\ p}{m}} = \frac{\frac{q\ A\ p}{m}}{\frac{p^2}{m}} \approx \frac{H_{I1}}{H_{particles}} << 1$$

intensity of X-ray source weak

spin order of magnitude

$$B = \nabla \times A, \quad |B| = ik\ A$$

$$\frac{H_{I2}^{spin}}{H_{I1}} = \frac{\frac{q}{m} h\ k\ A}{\frac{q}{m} p\ A} \approx \frac{a_0(1s)}{\lambda} << 1$$

X-ray photon ($\lambda \sim 1A$) interacts with core electron, with wavefunction highly concentrated close to nuclei

APPENDIX 3

$$\begin{cases} -\dfrac{\hbar^2}{2m}\dfrac{d^2}{dx^2}\Psi_2^* = E_2\Psi_2^* \\ -\dfrac{\hbar^2}{2m}\dfrac{d^2}{dx^2}\Psi_1 = E_1\Psi_1 \end{cases}$$

$$\begin{cases} x\,\Psi_1 \times \left[-\dfrac{\hbar^2}{2m}\dfrac{d^2}{dx^2}\Psi_2^* = E_2\Psi_2^* \right] \\ x\,\Psi_2^* \times \left[-\dfrac{\hbar^2}{2m}\dfrac{d^2}{dx^2}\Psi_1 = E_1\Psi_1 \right] \end{cases}$$

$$-\frac{\hbar^2}{2m}\int_{-\infty}^{+\infty}\left[x\,\Psi_1\frac{d^2}{dx^2}\Psi_2^* - x\,\Psi_2^*\frac{d^2}{dx^2}\Psi_1 \right] dx = (E_2 - E_1)\int_{-\infty}^{+\infty}\left[\Psi_2^*\, x\,\Psi_1\right] dx$$

APPENDIX 3

$$\int_{-\infty}^{+\infty}\left[x\,\Psi_1\frac{d^2}{dx^2}\Psi_2^* - x\,\Psi_2^*\frac{d^2}{dx^2}\Psi_1\right]dx = -\frac{2m}{\hbar^2}(E_2-E_1)\int_{-\infty}^{+\infty}\left[\Psi_2^*\,x\,\Psi_1\right]dx$$

(1) (2)

(1) $$\int_{-\infty}^{+\infty}\left[x\,\Psi_1\frac{d^2}{dx^2}\Psi_2^*\right]dx = \left[x\,\Psi_1\frac{d}{dx}\Psi_2^*\right]_{-\infty}^{+\infty} - \int_{-\infty}^{+\infty}\left[\Psi_1\frac{d}{dx}\Psi_2^*\right]dx$$

(2) $$\int_{-\infty}^{+\infty}\left[x\,\Psi_2^*\frac{d^2}{dx^2}\Psi_1\right]dx = \left[x\,\Psi_2^*\frac{d}{dx}\Psi_1\right]_{-\infty}^{+\infty} - \int_{-\infty}^{+\infty}\left[\Psi_2^*\frac{d}{dx}\Psi_1\right]dx$$

$$\left(-\int_{-\infty}^{+\infty}\left[\Psi_1\frac{d}{dx}\Psi_2^*\right]dx\right) - \left(\int_{-\infty}^{+\infty}\left[\Psi_2^*\frac{d}{dx}\Psi_1\right]dx\right) = -\frac{2m}{\hbar^2}(E_2-E_1)\int_{-\infty}^{+\infty}\left[\Psi_2^*\,x\,\Psi_1\right]dx$$

$$= \left[\Psi_1\Psi_2^*\right]_{-\infty}^{+\infty} - \left(\int_{-\infty}^{+\infty}\left[\Psi_2^*\frac{d}{dx}\Psi_1\right]dx\right)$$

APPENDIX 3

$$2\left(\int_{-\infty}^{+\infty}\Psi_2^*\frac{d}{dx}\Psi_1\quad dx\right)=-\frac{2m}{\hbar^2}(E_2-E_1)\int_{-\infty}^{+\infty}\left[\Psi_2^*\,x\,\Psi_1\right]dx$$

$$\int_{-\infty}^{+\infty}\left[\Psi_2^*\frac{d}{dx}\Psi_1\right]\quad dx=-\frac{m}{\hbar^2}(E_2-E_1)\int_{-\infty}^{+\infty}\left[\Psi_2^*\,x\,\Psi_1\right]dx$$

$$\int_{-\infty}^{+\infty}\left[\Psi_2^*\frac{d}{dx}\Psi_1\right]\quad dx=-\frac{m\omega}{\hbar}\int_{-\infty}^{+\infty}\left[\Psi_2^*\,x\,\Psi_1\right]dx$$

The absorption coefficient μ

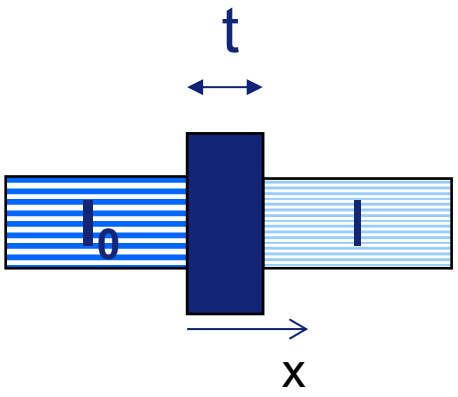

$$-dI = I(x)\, N \frac{dx}{t}\, \sigma_a$$

at/cm² cm²/at

$$-\int_0^t \frac{dI}{I(x)} = N \frac{\sigma_a}{t} \int_0^t dx$$

$$\ln I(t) - \ln I(0) = -N\sigma_a$$

$$\frac{I(t)}{I(0)} = e^{-N\sigma_a} = e^{-\mu t}$$

APPENDIX 4

$$\frac{I(t)}{I(0)} = e^{-N\sigma_a} = e^{-\mu t}$$

- μ is related to the atomic cross section:

$$\mu(\omega) = \sigma_a(\omega)\frac{N}{t} = \sigma_a(\omega)\frac{N_a}{A}\rho \qquad \left[\frac{cm^2}{at}\right] \frac{\left[\frac{at}{mole}\right]}{\left[\frac{gr}{mole}\right]} \left[\frac{gr}{cm^3}\right] = \left[cm^{-1}\right]$$

- in general you find tabulated the mass absorption coefficient μ/ρ:

$$\frac{\mu}{\rho} = \sigma_a \frac{N_a}{A} \qquad \left[\frac{cm^2}{at}\right] \frac{\left[\frac{at}{mole}\right]}{\left[\frac{gr}{mole}\right]} = \left[\frac{cm^2}{gr}\right]$$

- for a generic sample P_xQ_y…..:

$$\left(\frac{\mu}{\rho}\right)_{tot} = x\left(\frac{\mu}{\rho}\right)_P \frac{A_P}{M} + y\left(\frac{\mu}{\rho}\right)_Q \frac{A_Q}{M} + \ldots$$

Recipe for calculating t for transmission XAS

$$\frac{I(t)}{I(0)} = e^{-N\sigma_a} = e^{-\mu t}$$

1. Total absorption above the edge must not be too high:

   $\mu_{\text{above edge}}\, t = 2 \rightarrow 5$ $\qquad$ $I / I_0 \sim 0.14 \rightarrow 0.007$

   ideally $\qquad$ $\mu_{\text{above edge}}\, t = 2\text{-}3$

2. Contrast at edge must be as large as possible:

   $[\, \mu_{\text{above edge}} - \mu_{\text{below edge}} \,]\, t > 0.1$

   ideally $\qquad$ $[\, \mu_{\text{above edge}} - \mu_{\text{below edge}} \,]\, t = 1$

If absorber is very dilute, and matrix absorbs a lot, then this is not possible → fluorescence detection

Why complex numbers?

Real numbers allow you to work **only** in 1D. If you have a point at distance "a" from the origin, you only need one number to define its position:

a = length of the segment

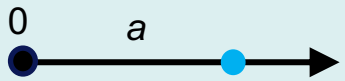

A **complex number** is a number that can be expressed in the form $a + ib$, where a and b are real numbers, and i is a solution of the equation $x^2 = -1$, which is called an imaginary number because there is no real number that satisfies this equation.

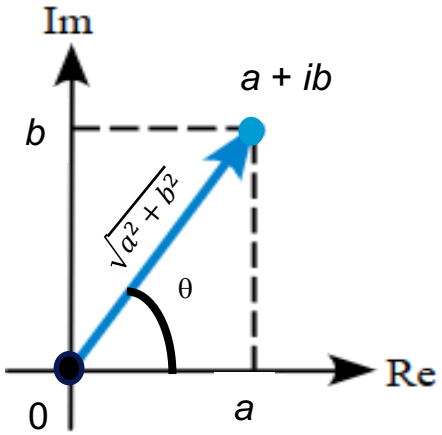

Complex numbers **allow you to work in 2D.** You need two numbers to define the position of a point on a plane:

- coordinate along x: *a*
- coordinate along y: *b*

OR

- length of segment: $\sqrt{a^2 + b^2}$
- angle with respect to x-axis: $\theta = \text{arctg}\,\frac{b}{a}$

$z = a + ib$

$z^* = a - ib$ → *"complex conjugate"*

a : real part → Re [z]

b : imaginary part → Im [z]

$|z|^2 = zz^* = a^2 + b^2$ → *"modulus square" or "amplitude"*

$\theta = \text{arctg}\,\frac{\text{Im}[z]}{\text{Re}[z]}$ → *"phase" or "argument"*

APPENDIX 5

The sum of a complex number z = a+ib and its conjugate z* = a-ib is equal to twice its real part: = z + z* = (a+ib) + (a-ib) = 2 a = 2 Re z

$$\mu(\omega) \propto \int d\vec{r} \left| \psi_i^*(\vec{r})\ \hat{\eta}\cdot\vec{r}\ [\ \psi_f^0(\vec{r}) + \delta\psi_f(\vec{r})\ ] \right|^2$$

$$\int d\vec{r} \left[\psi_i^*(\vec{r})\ \hat{\eta}\cdot\vec{r}\left(\psi_f^0(\vec{r}) + \delta\psi_f(\vec{r})\right)\right]\left[\psi_i(\vec{r})\ \hat{\eta}\cdot\vec{r}\left(\psi_f^{0*}(\vec{r}) + \delta\psi_f^*(\vec{r})\right)\right]$$

$$\left[\psi_i^*\psi_f^0 + \psi_i^*\delta\psi_f\right] + \left[\psi_i\psi_f^{0*} + \psi_i\delta\psi_f^*\right]$$

$$\left|\psi_i^*\psi_f^0\right|^2 + \left|\psi_i^*\delta\psi_f{}^2\right| + \left|\psi_i^*\delta\psi_f\psi_i\psi_f^{0*}\right| + \left|\psi_i^*\psi_f^0\psi_i\delta\psi_f^*\right|$$

$$\left|\psi_i^*\psi_f^0\right|^2 + \left|\psi_i^*\delta\psi_f{}^2\right| + 2\,\mathrm{Re}\left(\psi_i^*\delta\psi_f\psi_i\psi_f^{0*}\right)$$

MECHANISM AND KINETICS OF PT SINTERING AND REDISPERSION

ID24, ESRF

TOYOTA

5 years of research and development with Toyota

Design of completely new sample environment to comply with Toyota's needs

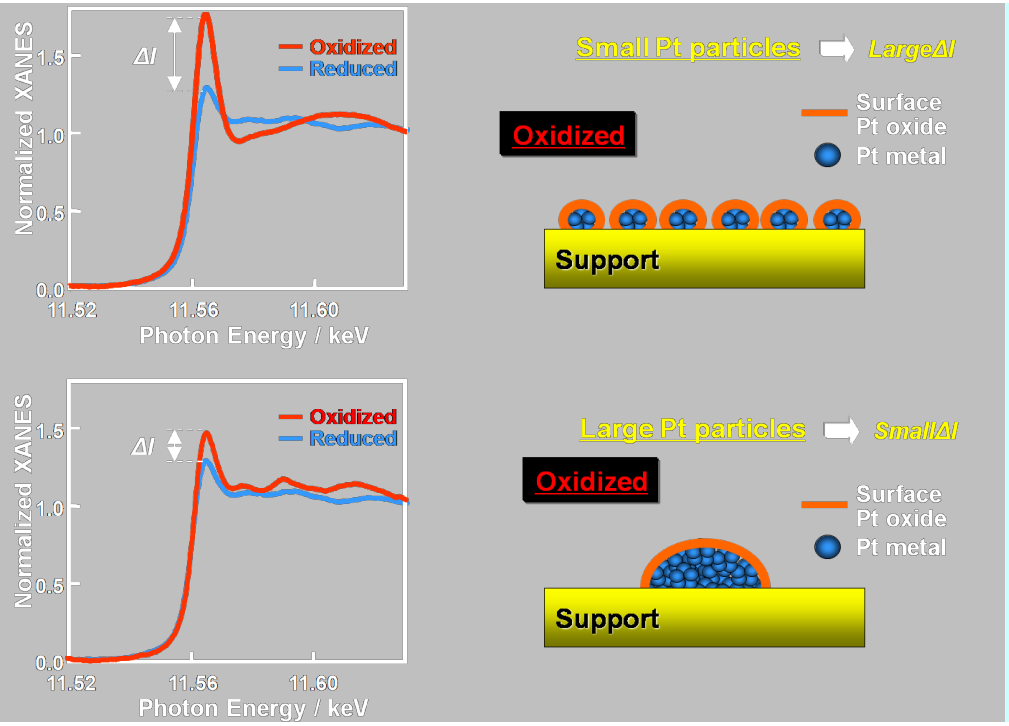

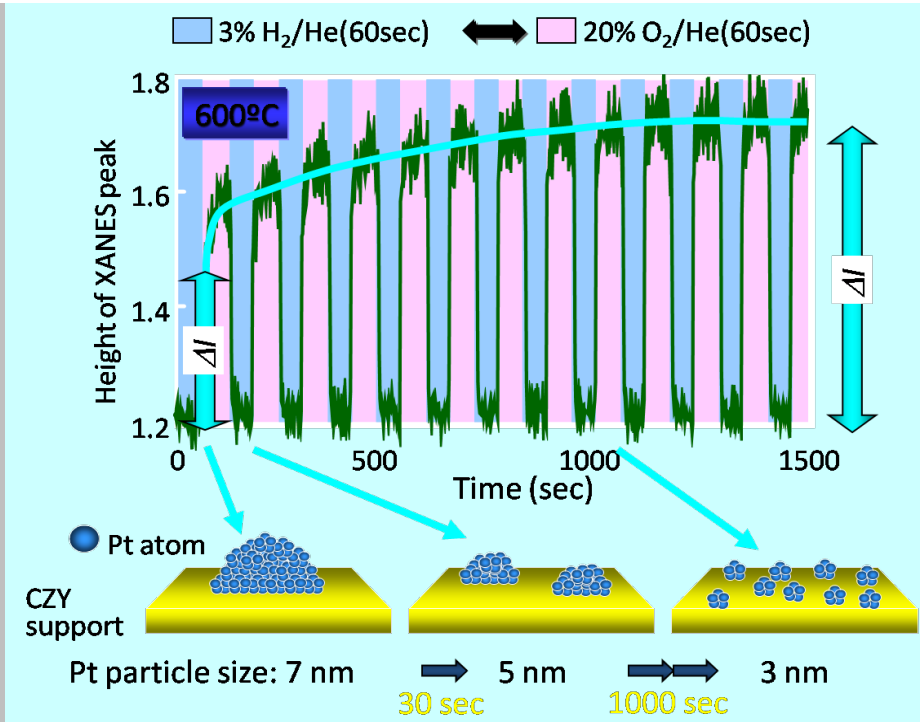

Establish mechanism and kinetics of Pt sintering and redispersion

Nagai Angew. Chemie 2008

OXYGEN DIFFUSION IN INDIVIDUAL CATALYST PARTICLE

GDCh **Communications** Angewandte International Edition Chemie

Heterogeneous Catalysis

International Edition: DOI: 10.1002/anie.201606046
German Edition: DOI: 10.1002/ange.201606046

Imaging of Oxygen Diffusion in Individual Platinum/$Ce_2Zr_2O_x$ Catalyst Particles During Oxygen Storage and Release

Hirosuke Matsui, Nozomu Ishiguro, Kaori Enomoto, Oki Sekizawa, Tomoya Uruga, and Mizuki Tada**

Angew. Chem. Int. Ed. 2016, 55, 1 – 5

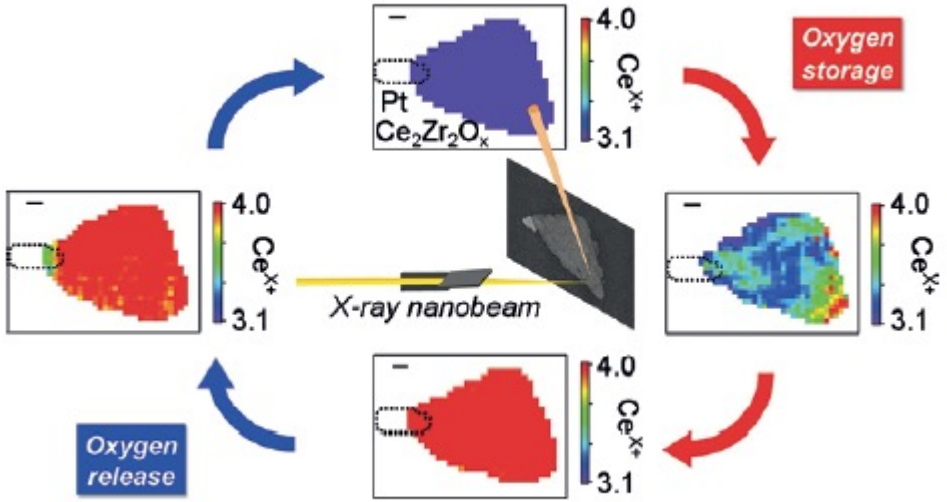

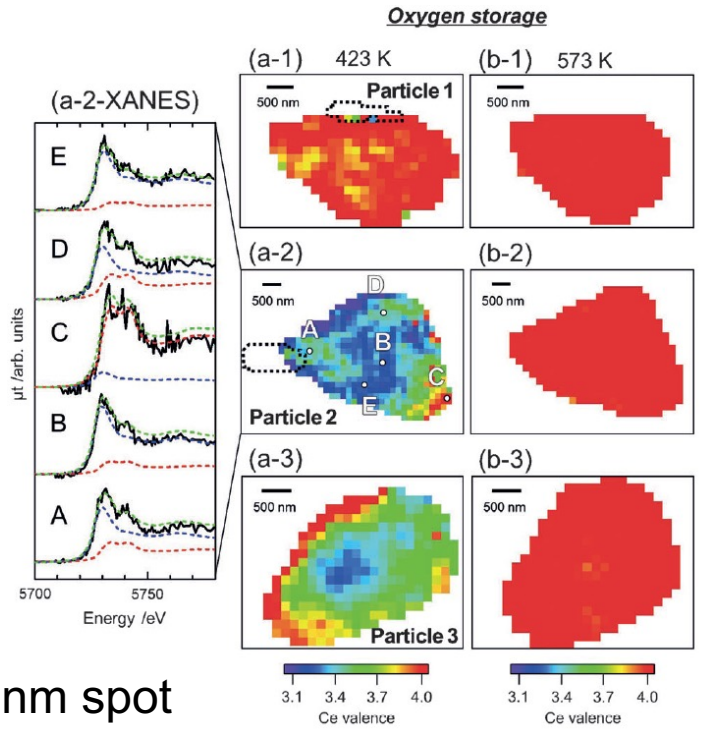

BL36XU, SPRING8

400 x 150nm spot

European XFEL

IN SITU AND *OPERANDO* XAS ON LITHIUM-ION BATTERY CATHODES

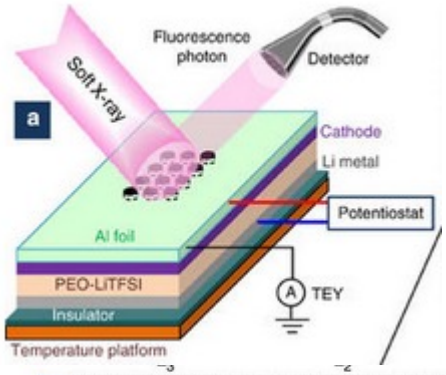

Ni $L_{2,3}$ XAS

8.0.1, ALS LBNL

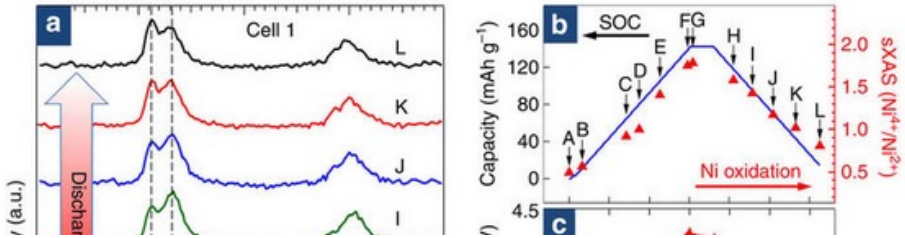

direct information of Ni oxidation state
→ element sensitive fingerprints of electrochemical process in Li-ion battery cathodes in real time

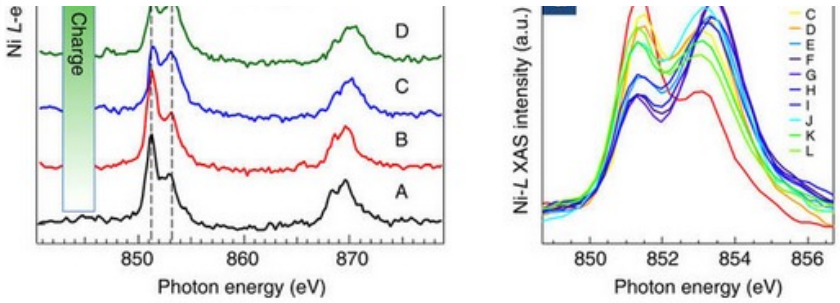

X. Liu et al. Nature Comm.4, 2568 (2013)

Ni K XAS

BM30B, ESRF

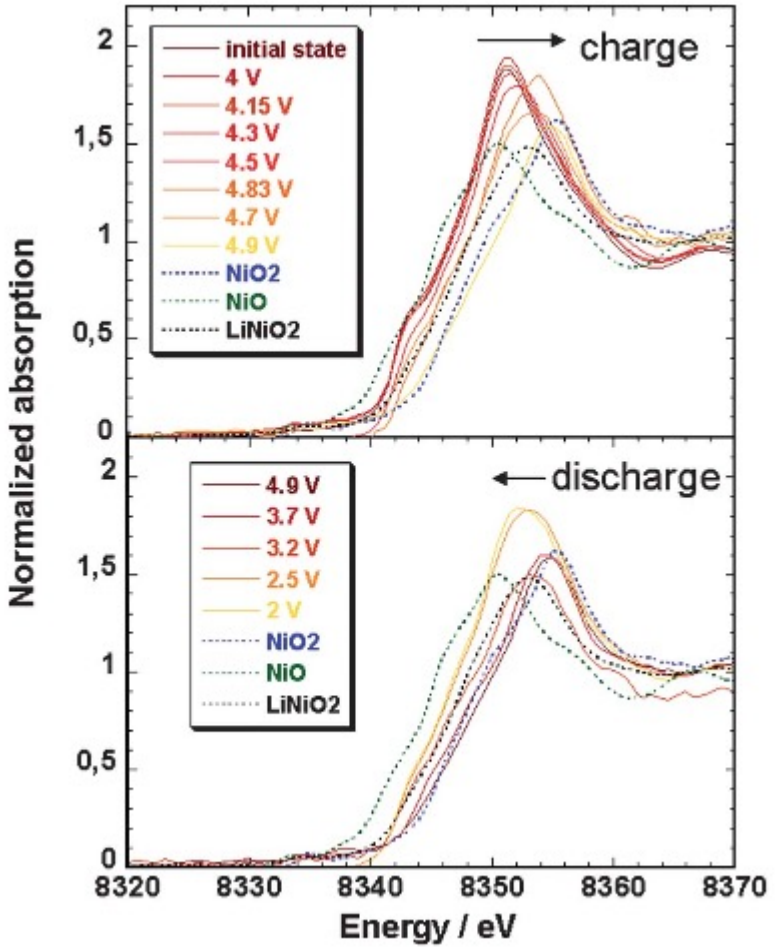

L. Simonin et al. J. Mater. Chem., 22, 11316 (2012)

CHARACTERIZATION OF SE IN UO2 SPENT NUCLEAR FUEL

Environmental Science
Processes & Impacts

ROYAL SOCIETY OF CHEMISTRY

PAPER

View Article Online
View Journal | View Issue

CrossMark click for updates

Cite this: *Environ. Sci.: Processes Impacts*, 2015, 17, 1760

Characterization of selenium in UO_2 spent nuclear fuel by micro X-ray absorption spectroscopy and its thermodynamic stability†

E. Curti,*[a] A. Puranen,[b] D. Grolimund,[a] D. Jädernas,[b] D. Sheptyakov[a] and A. Mesbah[cd]

microxas, SLS

- direct disposal of spent nuclear fuel in deep geological formations
- must assess to which extent radionuclides could be released to the environment

  → understand how they are chemically bound in the waste matrix

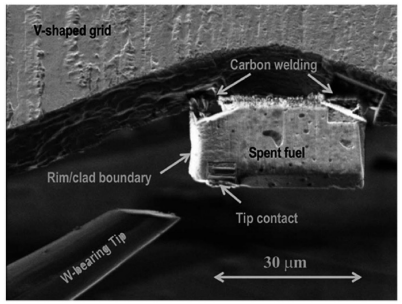

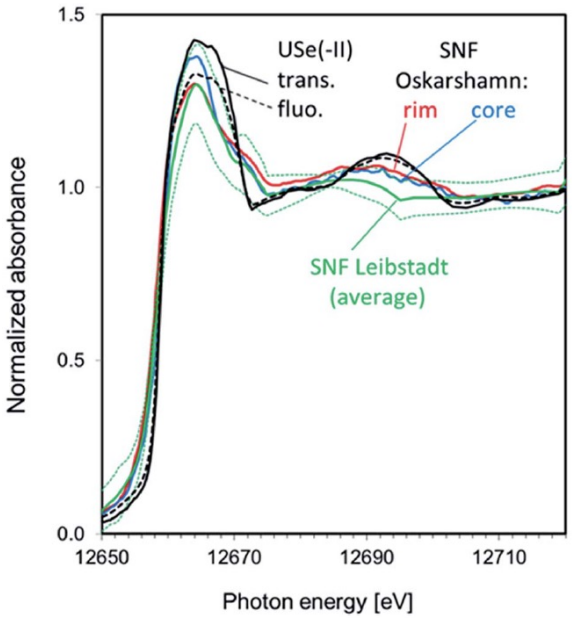

Se directly bound to U atoms as Se(II)

probably replacing O in the cubic UO_2 lattice

SURVIVAL OF FE-REDUCING BACTERIA UNDER ALKALINE CONDITIONS

GSECARS, APS

Sulfur-mediated electron shuttling during bacterial iron reduction

Theodore M. Flynn,[1,2] Edward J. O'Loughlin,[1] Bhoopesh Mishra,[1,3] Thomas J. DiChristina,[4] Kenneth M. Kemner[1]*

Science 344, 1039–1042, 2014

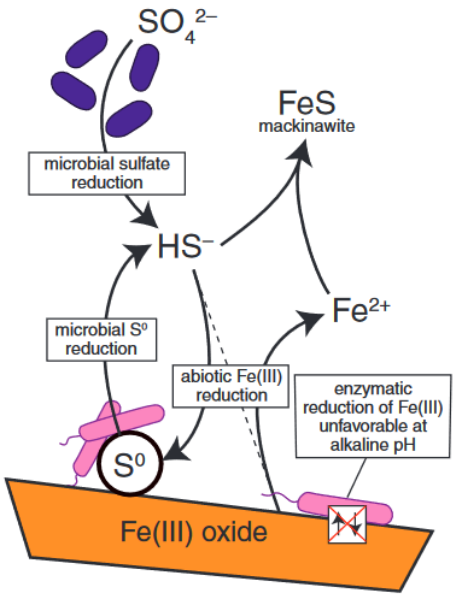

S- K XANES

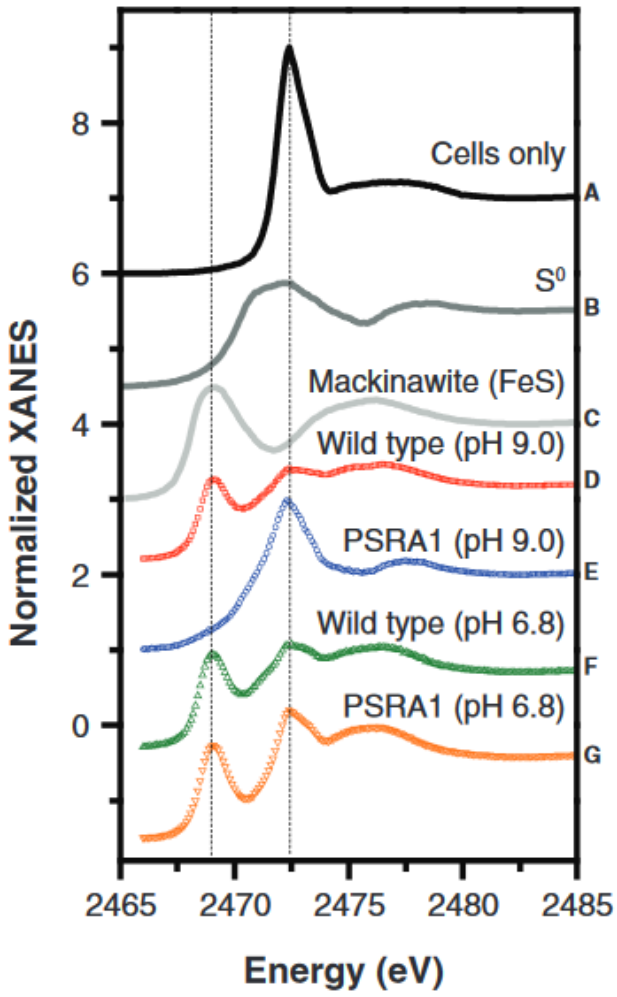

some Fe-reducing bacteria maintain S-reducing metabolic pathway, helping them survive under alkaline conditions

SHOCK COMPRESSED FE @ 5 MBAR, 15000K

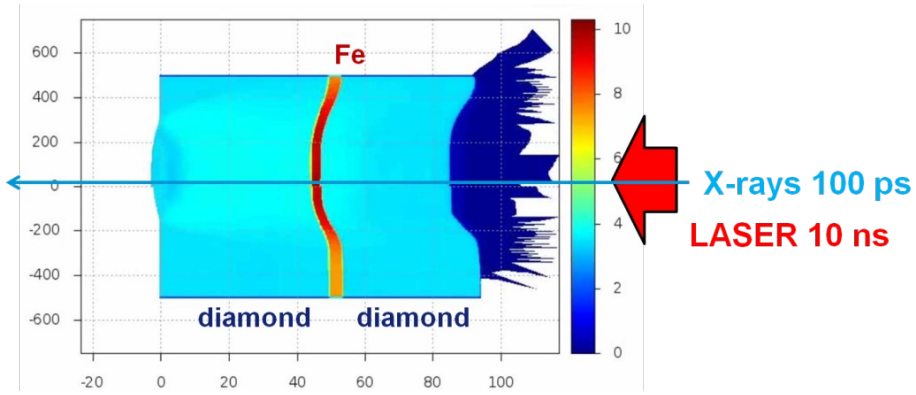

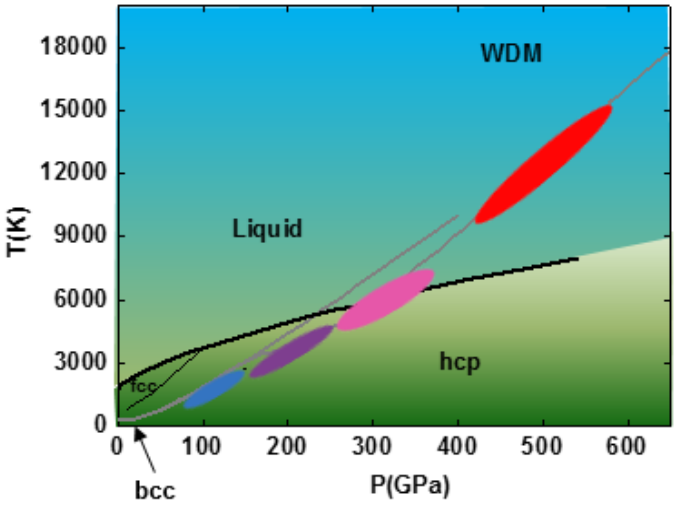

ID24, ESRF

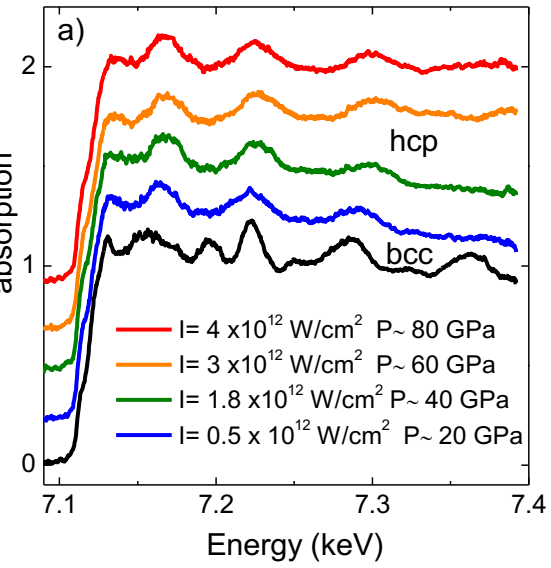

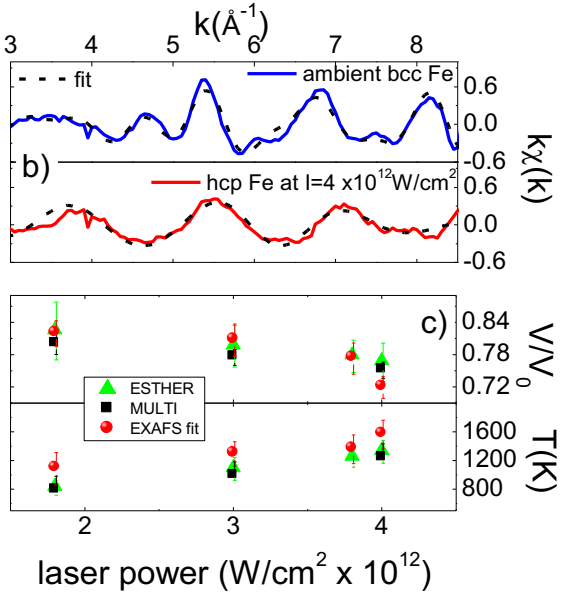

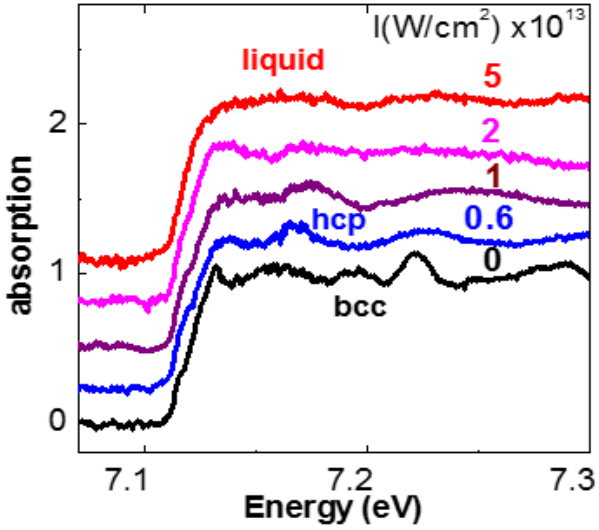

- Persistence of atomic correlations
- Discrepancy with theory on edge shift

European XFEL

Torchio Sci. Rep. 2016